TEKNOFEST 2022
ROCKET COMPETITION
Medium Altitude Category
Critical Design Report (CDR)
Presentation
EVA X

Team Structure

Asst. Prof. Doğu Çağdaş ATİLLA
ALTINBAŞ UNIVERSITY
Department of Electric and Electronics Engineering
Project Advisor

Sohaib ABOUALYAN
(Foreign student)
ALTINBAŞ UNIVERSITY
Mechanical Engineering
4th year student
Team Captain

Eda Nur GÖKSAL
ALTINBAŞ UNIVERSITY
Software Engineering
4th year student
Team Vice Captain

Bedirhan KÖKSOY
ALTINBAŞ UNIVERSITY
Computer Engineering
2nd year student
Software Team Member

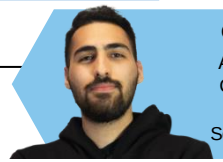

Gökhan EVLEK
ALTINBAŞ UNIVERSITY
Computer Engineering
2nd year student
Software Team Member

Kaan Avcı
ALTINBAŞ UNIVERSITY
Electric-Electronic Engineering
1st year student
Electric Team Member

Osamah HAMMOODI
(Foreign student)
ALTINBAŞ UNIVERSITY
Mechanical Engineering
4th year student
Mechanical Team Member

Pelin Tüfekçi
ALTINBAŞ UNIVERSITY
Industrial Engineering
Prep year student
Mechanical Team Member

Ömercan LİMLİ
ALTINBAŞ UNIVERSITY
Mechanical Engineering
3rd year student
Mechanical Team Member

Rabia Kazaz
ALTINBAŞ UNIVERSITY
Industrial Engineering
Prep year student
Mechanical Team Member

Competition Rocket General Information

About the Competition Rocket General Information

	Measure
Length (mm):	3090
Diameter (mm):	130
Dry Weight of Rocket (g):	19781
Fuel Mass (g):	4349
Engine Dry Weight (g):	2683
Payload Weight (g):	4158
Total Takeoff Weight (g):	26813

Table 1. EVA X-1 General Information.

Predicted Flight Data and Analyses

	Measure
Takeoff Thrust/Weight Ratio:	7.69:1
Ramp Ascent Speed (m/s):	33.00
Stability (for Mach 0.3):	1.57
Maximum acceleration (g)	9.29
Maximum Velocity (m/s):	280.43
Highest Mach Number:	0.84
Apogee (m):	3395.00

Table 2. EVA X-1 Open Rocket Simulation Data.

Engine

Cesaroni M2020

Table 3. EVA X-1 Rocket Engine.

General Design

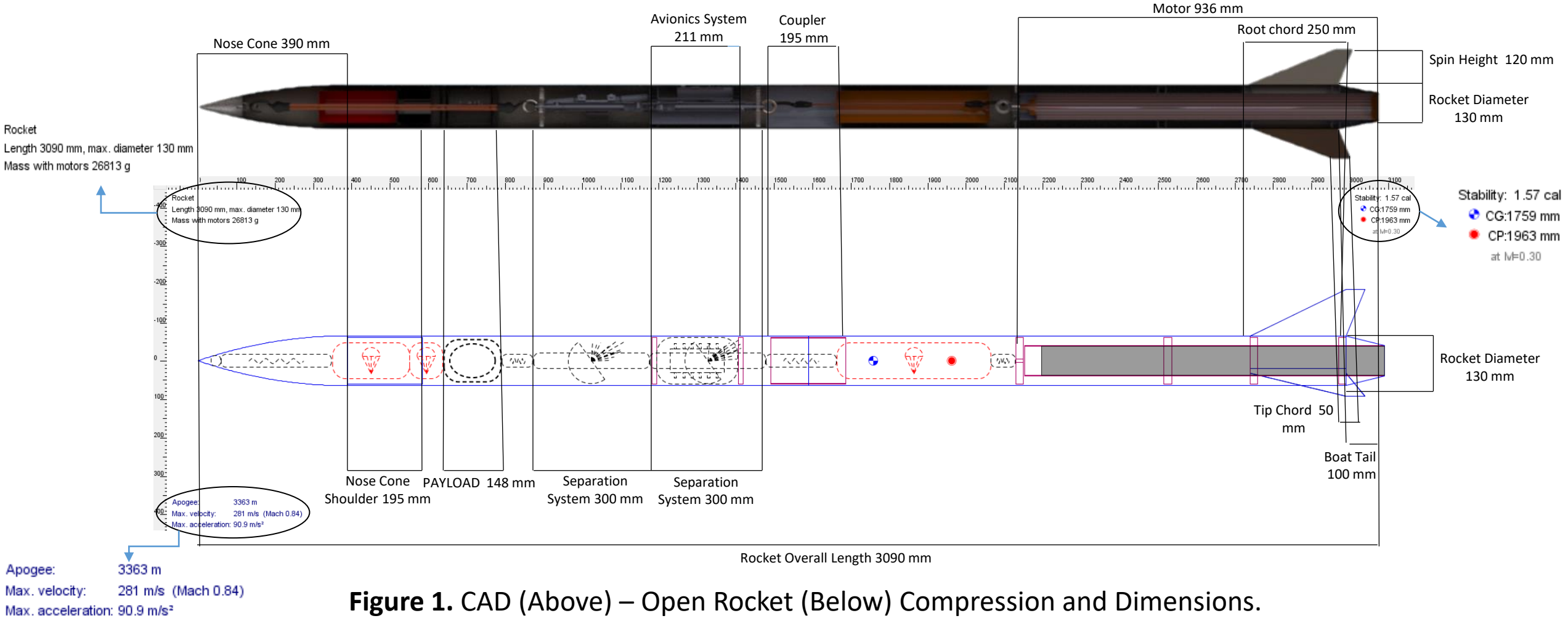

Figure 1. CAD (Above) – Open Rocket (Below) Compression and Dimensions.

Operation Concept (CONOPS)

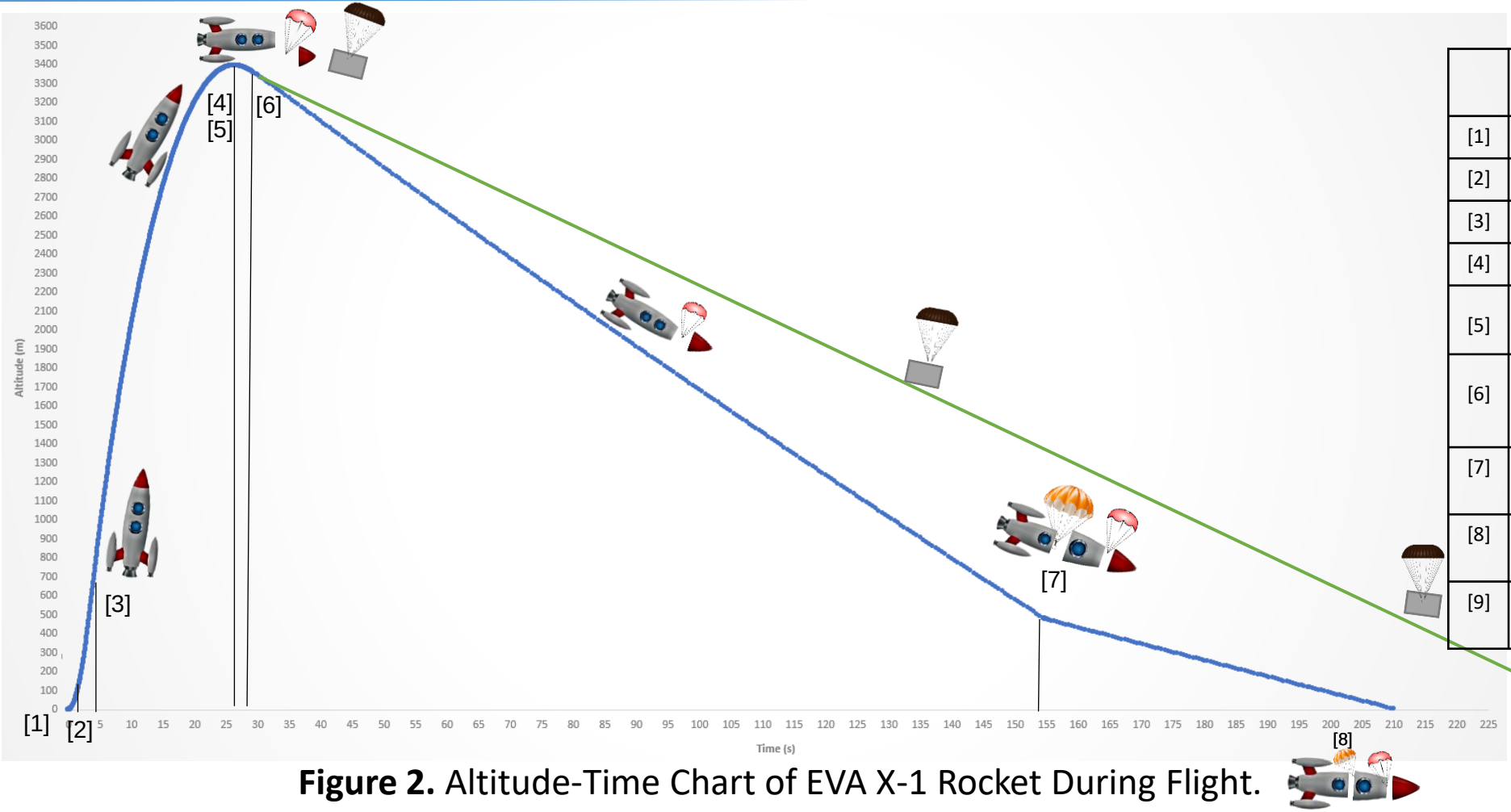

Figure 2. Altitude-Time Chart of EVA X-1 Rocket During Flight.

Table 4. Flight profile.

		Time (s)	Altitude (m)	Velocity (m/s)
[1]	Launch	0.00	0.00	0.00
[2]	Rail Tip	0.40	6.00	33.02
[3]	Motor Burn Out	4.32	756	274.79
[4]	Apogee	26.30	3395.00	12.30
[5]	Drogue Parachute Deployment	26.30	3395.00	12.30
[6]	PAYLOAD/PAYLOAD Parachute Deployment	29.30	3357.75	20.21
[7]	Main Parachute Deployment	153.77	493.60	21.46
[8]	Rocket Ground Hit	211.00	0.00	8.49
[9]	PAYLOAD Ground Hit	373.21	0.00	10.53

PDR - CDR Changes - 1

Table 4.1. PDR - CDR Changes – 1.

Subject of Change	On Which Page in the PDR?	What Was The Content in PDR	What Happened to the Content in the CDR?	On which Page in CDR?
Team Structure	2	Team members .	Three members have been replaced with new ones.	2
Competition Rocket General Information	3	PDR Tables 1. and 2.	CDR Tables 1. and 2.	3
General Design	4	Rocket general open rocket details.	Rocket general open rocket details.	4
Flight Profile Table	5	Table 4. Flight Profile.	Table 4. Flight Profile.	5
PAYLOAD Parachute color	22	Brown.	Black.	35
PAYLOAD mass	25	4000 g.	4158 g.	38
Recovery system	19	1 Piston used for recovery.	2 Pistons with different dimensions are now used.	31-34
Recovery activation system	19	Pyrobolt used to activate CO_2	Servo Motor and CO_2 Inflators used to activate .	33
PAYLOAD	25	Dimensions Figure 15.	Dimensions Figure 33.	38

PDR - CDR Changes - 1

Table 4.2. PDR - CDR Changes - 1

Subject of Change	On which page in the PDR?	What was the content in PDR	What happened to the content in the CDR?	On which page in CDR?
Boat Tail	15	Wall thickness Figure 10.	Wall thickness Figure 14.	18
Parachute	22	Spill Hole Area.	Spill Hole Area is now 20% of the parachute open diameter.	36
Main avionics and backup avionics sensors	26	BMP180 MPU6050	MPU6050 BMP180	46
Main avionics and payload GPS	24,28	GY-NEO 6M GPS	Grove - GPS (Air530)	39,49
Main avionics and backup avionics processor and card	26	ATmega328PU and Arduino Uno	ATmega2560 and Arduino Mega Pro Mini	46
Backup Avionics Telemetry	32	XBee S3B Pro	DRF7020D27	55

PDR - CDR Changes -2nd

Table 5.1. PDR - CDR Changes -2nd

Subject of Change	New Content Topic?	Content Detail in CDR?	Which Page in the CDR?
Main Avionics and Backup Avionics Sensors	The main avionics pressure sensor was replaced with the IMU sensor and the backup avionics IMU sensor with the pressure sensor.	The IMU and pressure sensors between the two avionics were replaced, since it was determined that the main avionics computer had triggers other than pressure, which facilitated separation.	46
Main avionics and payload GPS	The GY-NEO 6M GPS in the main avionics and payload has been replaced by the Grove GPS (Air530).	Since the GY-NEO 6M GPS module could not operate at the desired performance, it was switched to the Grove GPS (Air530) module.	39,49
Main Avionics and Backup Avionics Processor and Card	The Atmega328PU processors with Arduino Uno in the main avionics and backup avionics have been replaced by the ATmega2560 with Arduino Mega Pro Mini.	Since the ATmega328PU processor with Arduino Uno card do not have enough pins, multi-pin the ATmega2560 processor with Ardunio Mega Pro Mini are preferred.	46
Backup Avionics Telemetry	Replaced the XBee S3B Pro module in the backup avionics with the DRF7020D27.	Since the Xbee S3B Pro module is not available in Turkey, it has been replaced to the DRF7020D27 module.	55
Avionics Computers Battery	Battery information has been added to the avionics computers section.	Detailed information was given about avionics batteries.	46
Avionics Computers and PAYLOAD Antenna	Antenna information has been added to the avionics computers section.	Detailed information about avionic antennas was given.	39,46

PDR- CDR Changes -2nd

Table 5.2. PDR - CDR Changes -2nd

Subject of Change	New Content Topic?	Content Detail in CDR?	Which Page in the CDR?
Ground Station Processors	Ground Station Processors types information has been added to the ground station section.	Detailed information about ground station processors was given.	60
Ground Station Telemetry Modules	Ground Station Processors types information has been added to the ground station section.	Detailed information about ground station telemetry modules was given.	60
Separation Activation System	The activation system used to activate the separation has been changed	The detailed activation system used to activate the separation are servo motor and CO_2 inflators	32

Flight Simulation Report (FSR)

Flight Simulation Report (FSR) is located in a zip file in pdf format.

Mass Budget

Mass Budget is located in a zip file in excel format.

Rocket Subsystem Details

Nose Cone Mechanical View

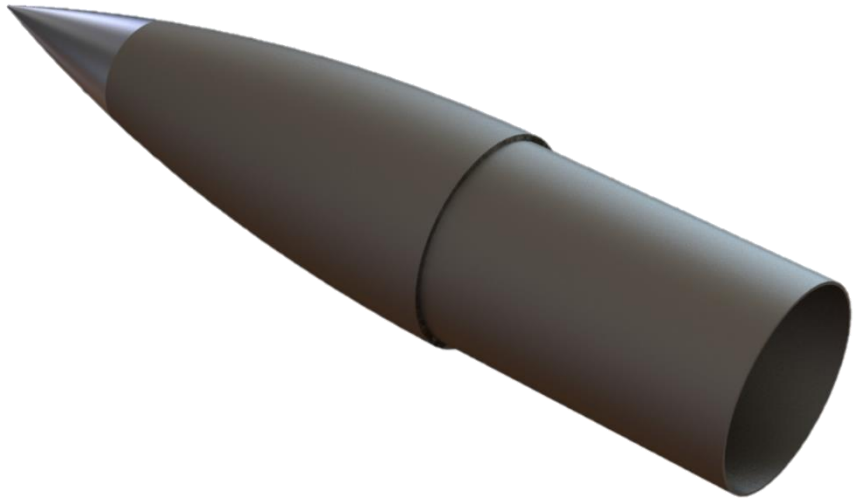

Figure 3. Nose Cone 3D View (CAD).

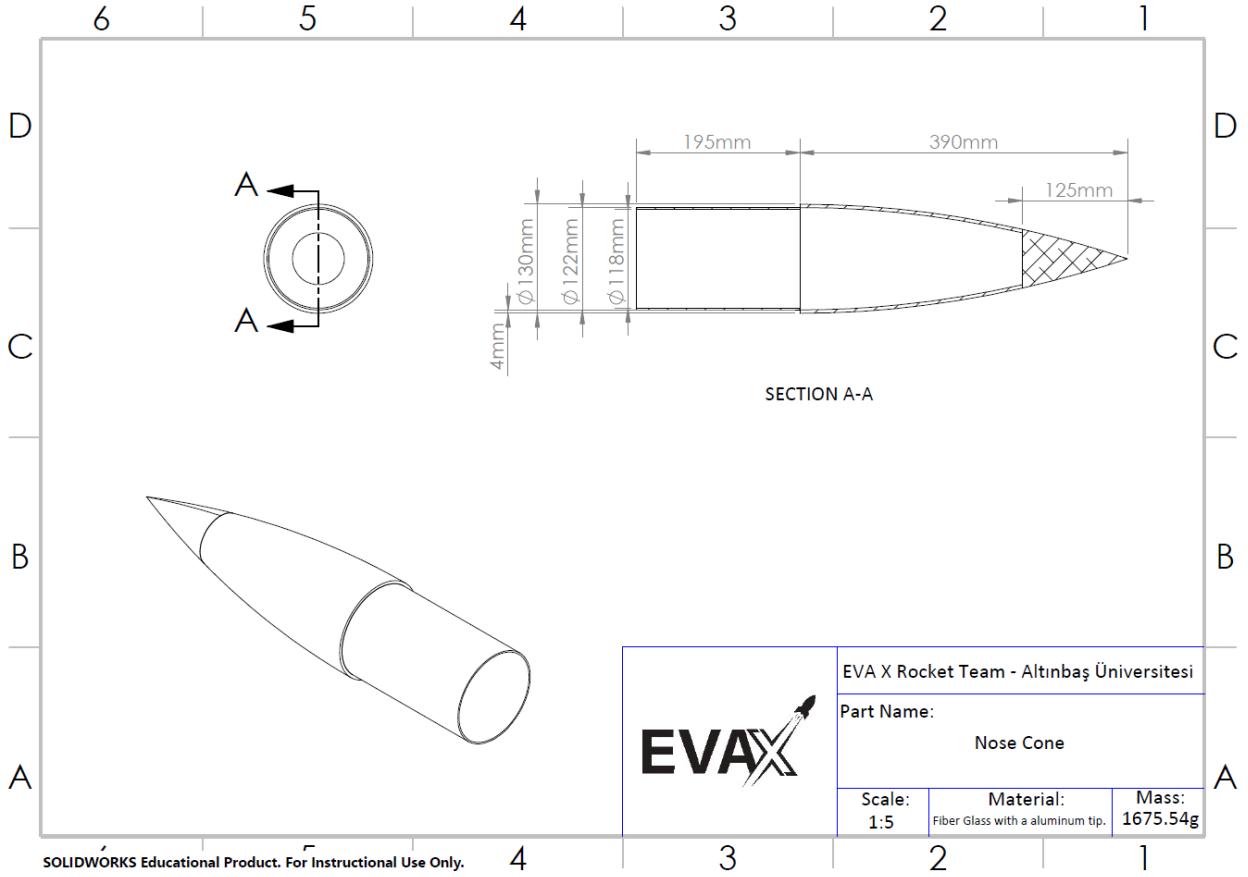

Figure 4. Nose Cone Technical Drawing.

Nose Cone –Detail

Table 6. Nose Cone Material Property [8,9,10].

Feature	Part	Elastic modulus (GPa)	Manufacturing
E-Glass Fiber	Nose cone (without tip)	72.3	Medium difficulty
Carbon Fiber	-	230	Medium difficulty
7075 T6 Aluminum	Nose cone tip	71.7	Hard and expensive

- When choosing the material for the nose cone, the strength, durability, and heat resistance that the material must withstand during flight were all taken into consideration. As a result, we chose E-fiber glass as the primary material since it outperformed carbon fiber in terms of not blocking RF signals and being robust enough to withstand flight pressures, as well as having a lower density than carbon fiber and aluminum.
- Because the tip of the nose cone absorbs the greatest heat during flight and aluminum is a superior material when it comes to heat resistance, it was decided to go with a 7075 T6 Aluminum at the tip of the nose cone.

Nose Cone –Detail

Table 7. Nose Cone Production Method.

Production Method	Production Capability	Explanation
CNC Aluminum Nose Cone then produce a mold and Vacuum.	Hard and Expensive	An Aluminum cut of our nose cone shape would be produced by CNC cutting then a mold will be produced from fiber glass and polyester resin. Hand laying, with the number of layers desired, of Fiber Glass/Epoxy will then be done to the polyester mold produced and vacuumed.
3D Printed Nose cone Mold and Vacuum.	Easy and Cheap	A mold has been made from the CAD of the nose cone and then 3D printed. The PLA printed mold had a 50% fill and a 1.2mm wall thickness to make sure it can handle the vacuum process it will go through. Hand laying is then done, with the number of layers desired, from Fiber Glass/Epoxy and finally vacuumed and placed in the oven to dry. This method is cheaper and easier as the mold is immediately printed instead of producing an expensive Aluminum nose cone. For the nose cone tip however it will be CNC cut from Aluminum as the part is small and wont cost much to manufacture.

To draw the nose cone curve, for the mold, in SolidWorks we used an equation driven curve using the parabolic nose cone formula (1) shown below. The nose cone shoulder was then added at the end of the nose cone with a length of 1.5*diameter of the rocket.

$$y = R\left(\frac{2\left(\frac{x}{L_n}\right) - K'\left(\frac{x}{L_n}\right)^2}{2 - K'}\right) \quad (1)\ [3]\ ,$$

L_n (length of nose cone) set as 390 mm
R_n (Base radius of nose cone) set as 65 mm
K’ (Parabola type constant) set as 1

So, $y = 65\left(\frac{2\left(\frac{x}{390}\right) - 1\left(\frac{x^2}{390}\right)}{2-1}\right), y = \frac{1}{3}x - \frac{x^2}{2340}$

Simplified Quadratic Equation used for the nose cone mold curve.

Fins Mechanical Appearance

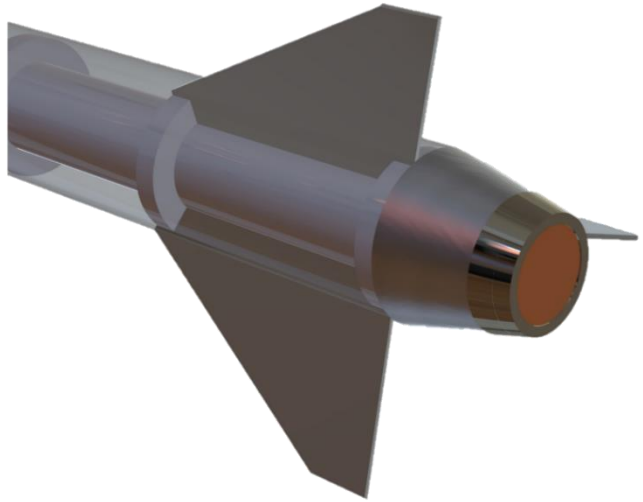

Figure 5. Fin 3D View (CAD), Assembled.

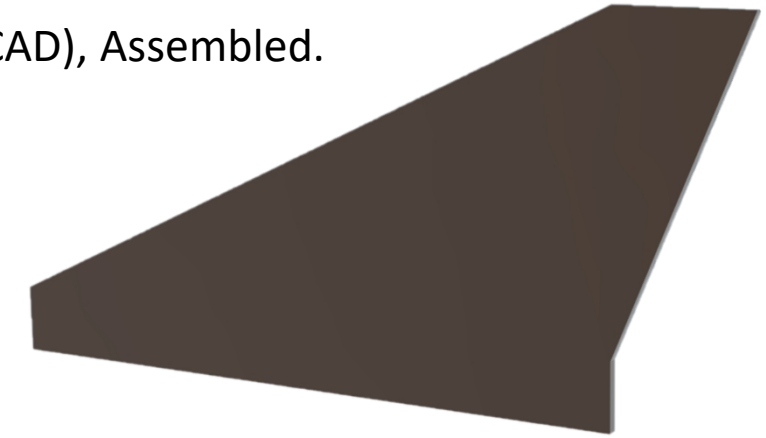

Figure 6. Fin 3D View (CAD), Singular.

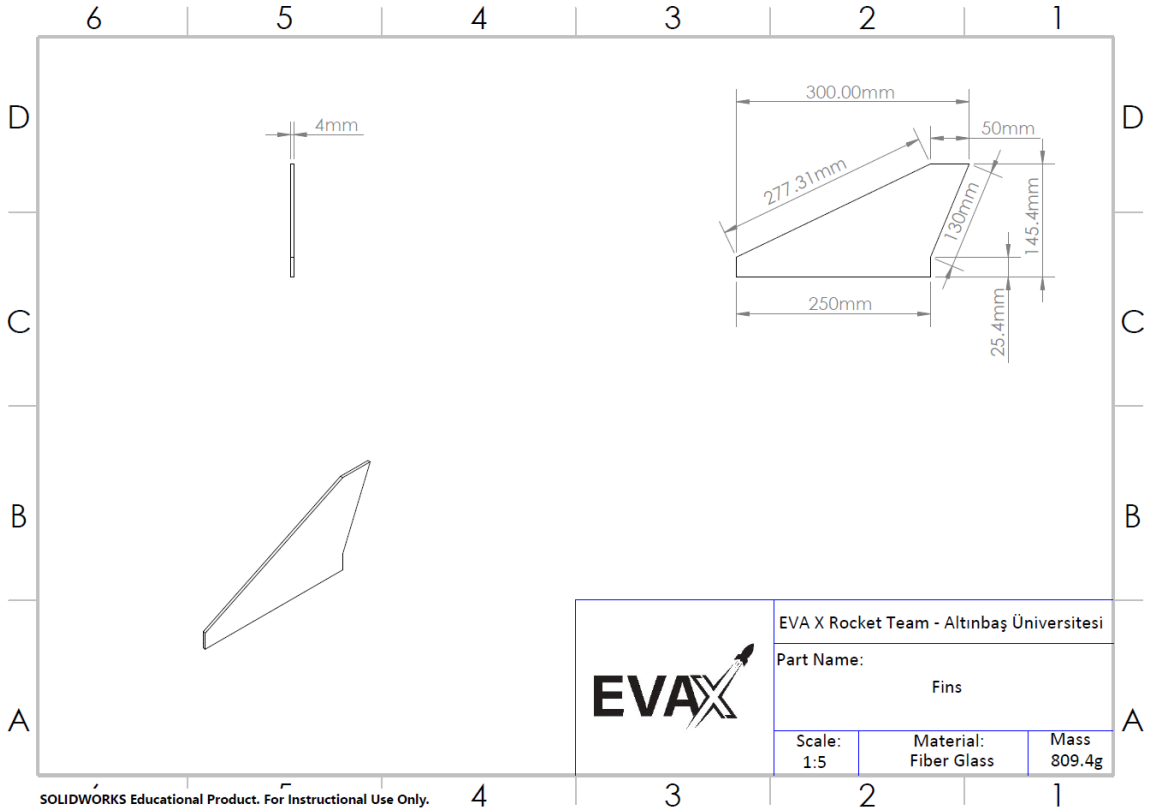

Figure 7. Fin Technical Drawing.

Fins –Detail

Table 8. Fins Material Property [8,9,10,11].

Feature	Elastic modulus (GPa)	Manufacturing
E-Glass Fiber	72.3	Medium difficulty
Carbon Fiber	230	Medium difficulty
7075 T6 Aluminum	71.7	Expensive
Plywood	8.30	Cheap and Easy

- Because the fins will be subjected to significant drag forces during flight, the material utilized must be strong enough to withstand such forces while yet being light enough to avoid causing damage to the frame body. E-Glass Fiber was chosen with these considerations in mind.
- A 3 mm block of E-Glass Fiber will be purchased, and water jet cut into the necessary shape as shown in Figure 7's technical drawing. Water jet cutting has been chosen as better suited to cutting fiber glass blocks than a CNC machines. The generated Fins will have sharp edges, which will increase the drag acting on the fins. To reduce the drag acting on the fins, we will add an epoxy fillet to the sharp edges.

Body Parts & Body Assembly Parts (STRUCTURAL) Mechanical View

Figure 8. Primary Frame 3D View (CAD).

Figure 9. Main Frame 3D View (CAD).

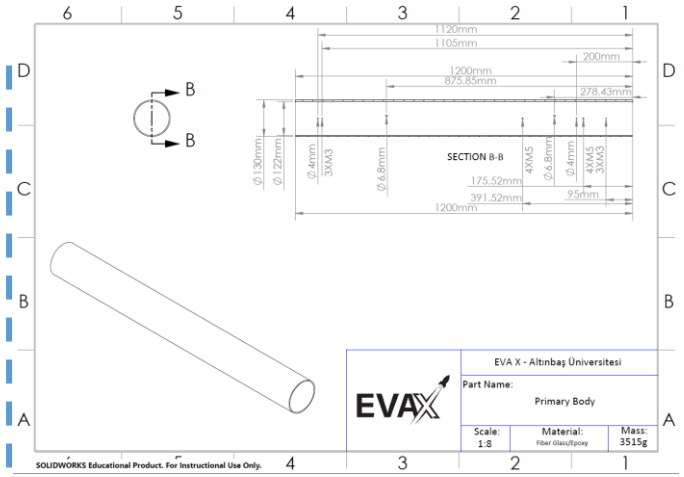

Figure 10. Primary Frame Technical Drawing.

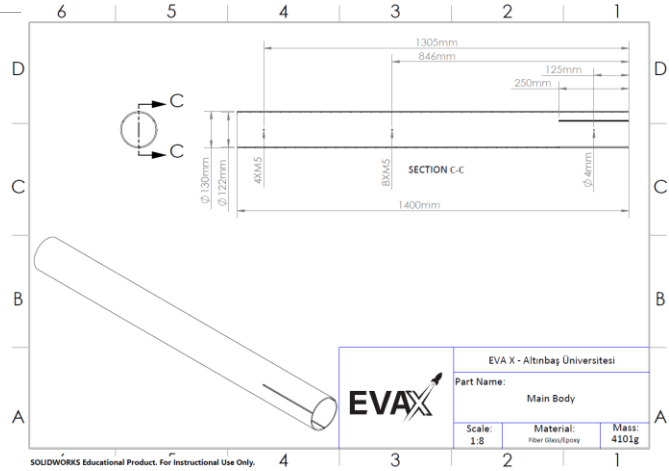

Figure 11. Main Frame Technical Drawing.

Body Parts & Body Assembly Parts (STRUCTURAL) Mechanical View

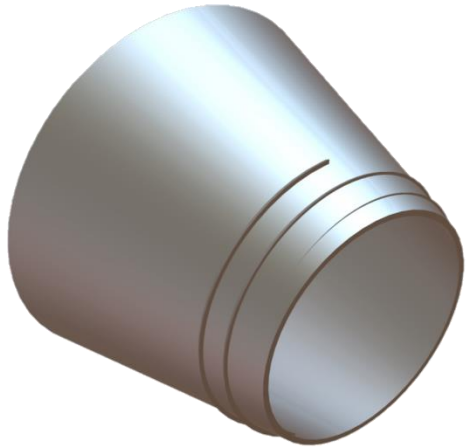

Figure 12. Boat Tail 3D View (CAD).

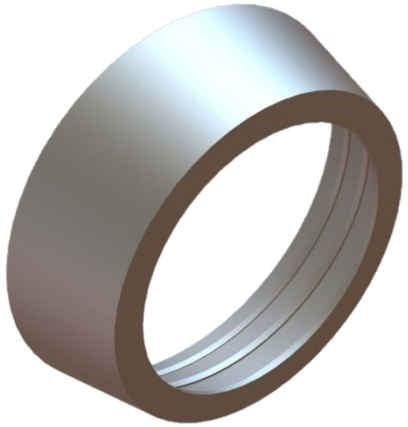

Figure 13. Engine Retainer 3D View (CAD).

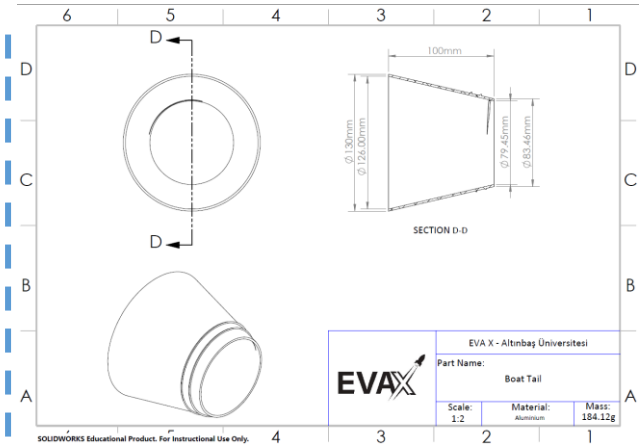

Figure 14. Boat Tail Technical Drawing.

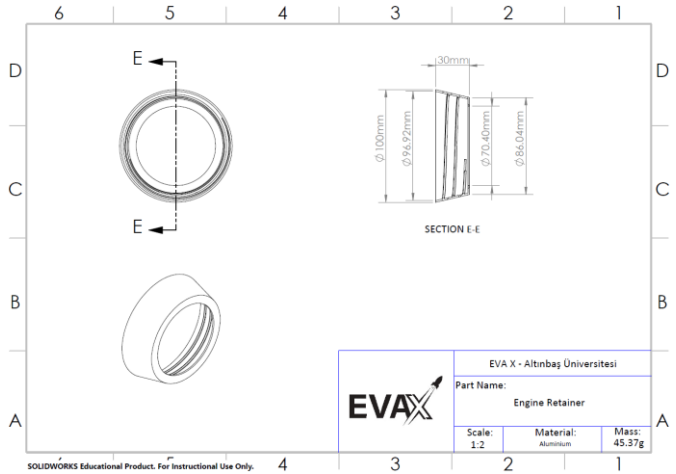

Figure 15. Engine Retainer Technical Drawing.

Structural – Body Parts

Table 9. Structural – Body Parts Material Property [8,9,10].

Feature	Part	Elastic modulus (GPa)	Manufacturing
E-Glass Fiber	Rocket Frames	72.3	Medium difficulty
Carbon Fiber	-	230	Medium difficulty
7075 T6 Aluminum	Boat Tail	71.7	Hard and Expensive

- For the rocket frames' core material has been chosen as E-Glass Fiber since it has the lowest density of all the materials and is still robust enough to withstand flight stresses. Furthermore, Fiber Glass will not interfere with the transmission of RF signals from our avionics system to the ground station and sensor systems, which is critical to the success of our rocket. Two samples of fiber glass and carbon fiber were manufactured and tested using compression testing to see if fiber glass could resist the pressures of flight. Fiberglass was able to withstand a force of roughly 50 kN.
- For the Boat Tail and Engine Retainer 7075 T6 Aluminum was chosen since they will be influenced by the heat generated by the motor during launch.

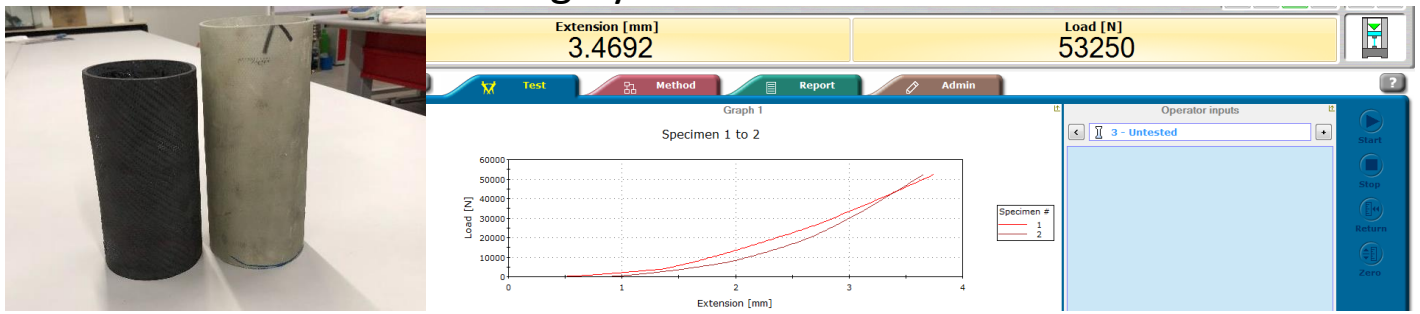

Figure 16. E-Glass Fiber (1) – Carbon Fiber (2) Sample Compression Test.

Structural – Body Parts

Table 10. Structural – Body Parts Production Method.

Production Method	Production Capability	Explanation
Male and Female Mold	Very Hard and Expensive	An aluminum tube with a outside diameter of 130 mm would be parachuted and prepared to make a 2 female molds from them using Fiber Glass and polyester resin. Once the molds are ready, we would hand lay, with the number of layers desired, on them using Fiber Glass/Epoxy and vacuum after.
Male Mold	Hard and less costy	An aluminum tube with a outside diameter of 122 mm has been purchased to be used as our mold. After placing none stick plastic on the mold hand laying of Fiber Glass/Epoxy is done with the desired number of layers to give us the outside diameter of 130 mm. While the Fiber Glass/Epoxy is drying, the frame will be vacuumed to make it stronger. This method is cheaper and easier than the one stated above so with that in mind we selected it.
CNC Aluminum	Costy	The boat tail and engine retainer will be made from aluminum and CNC cut as desired.

- Two pressure holes with a diameter of 4 mm will be included in the Primary Frame. A pair of three M3 thread holes will also be drilled for shear pins to be broken by the separation systems. Another set of four M5 thread holes will be drilled into the rocket to mount the avionics system and separation systems. Two 6.8 mm holes will be drilled within the body to accommodate rotating switches for the payload and avionics computer.
- The Main Frame will include four M5 thread holes for mounting the coupler and eight M5 thread holes for mounting the engine block. For pressure, another 4 mm diameter hole will be drilled between the fins. Finally, two 4 mm holes will be drilled for the rail bottoms on each body, one at the beginning of the fins and the other under the avionics. Figures 10 and 11 show all these perforations.

Structural – Body/In-Body Structural Supports (Integration Bodies, etc.)

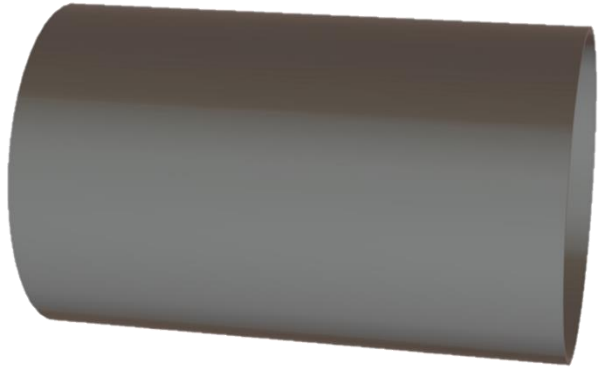

Figure 17. Coupler 3D View (CAD).

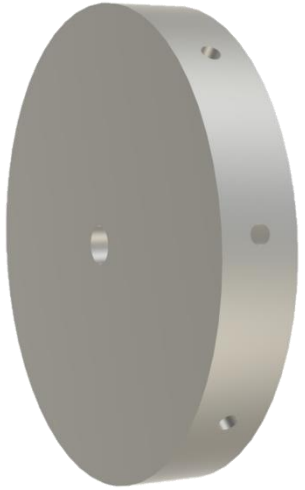

Figure 18. Engine Block 3D View (CAD).

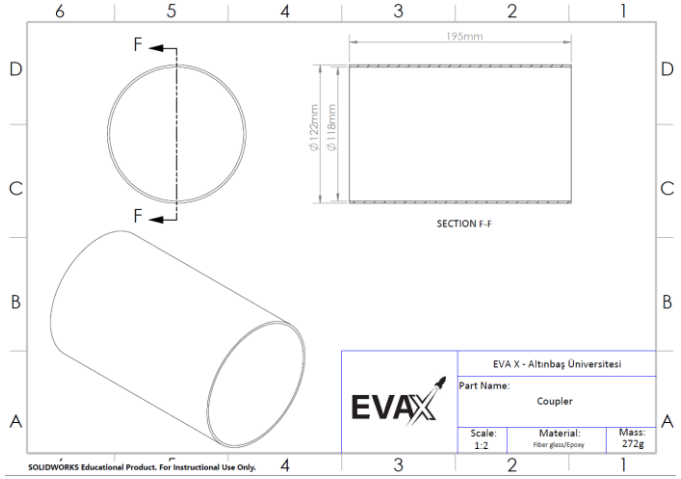

Figure 19. Coupler Technical Drawing.

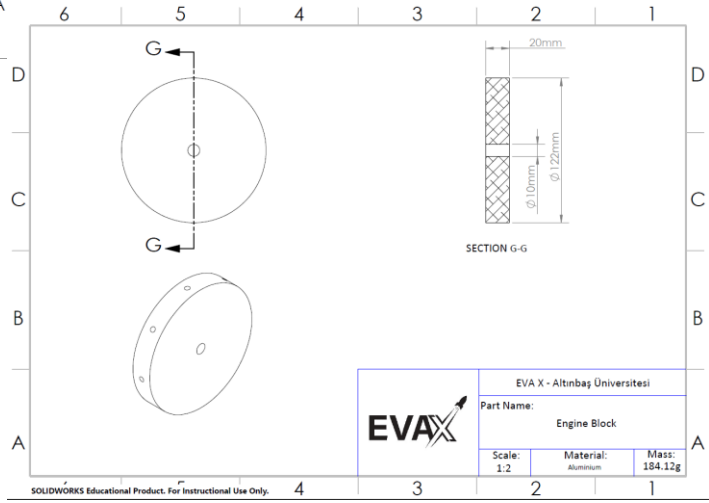

Figure 20. Engine Block Technical Drawing.

Structural – Body/In-Body Structural Supports (Integration Bodies, etc.)

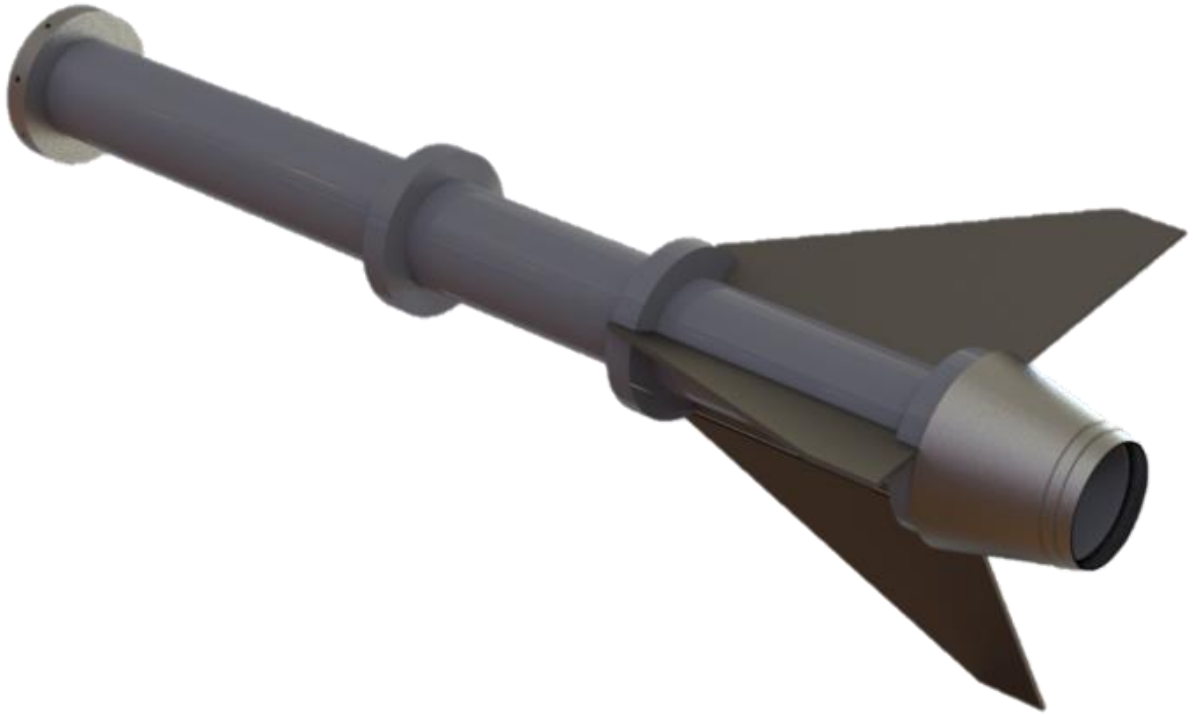

Figure 21. Engine Block One-Piece 3D View (CAD).

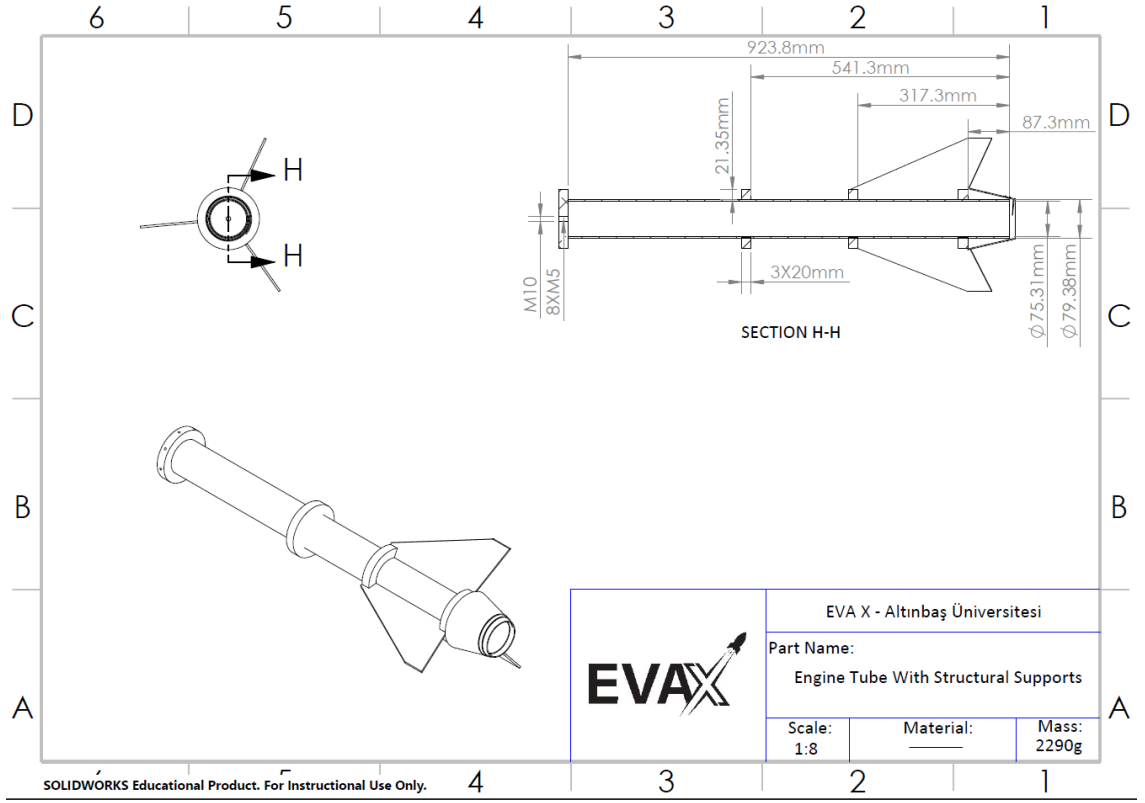

Figure 22. Engine Block One-Piece Technical Drawing.

Structural – Body/In-Body Structural Supports (Integration Bodies, etc.)

Table 11. Structural – Body/In-Body Structural Supports Material Property[8,9,10,11].

Feature	Part	Elastic modulus (GPa)	Manufacturing
E-Glass Fiber	Coupler	72.3	Medium difficulty
Carbon Fiber	-	230	Medium difficulty
7075 T6 Aluminum	Engine Blocks and Centering Rings	71.7	Hard and Expensive
Plywood	Centering Ring	8.3	Cheap and Easy

- The coupler will be made of the same material (E-Fiber Glass/Epoxy) as the Primary and Main Frames for the same reasons, as E-Glass Fiber is strong enough to handle the forces to it and light at the same time compared to other materials.
- The engine block, on the other hand, will be made of 7075 T6 Aluminum because it will have the motor right under it and will hold the rocket together, using an M10 eyebolt screwed into it, so it must be strong and heat resistant.
- The engine tube will be constructed of E-Glass Fiber, and the centering rings will be mounted around it to hold the fins and boat tail in place. A centering will be made of Plywood while the other two that will hold the fins and boat tail will be made of 7075 T6 Aluminum to assure a strong mount is done between the bodies.

Structural – Body/In-Body Structural Supports (Integration Bodies, etc.)

Table 12. Structural – Body/In-Body Structural Supports Production Method.

Production Method	Production Capability	Explanation
Male Mold	Medium	A male Aluminum tube with an outside diameter of 75.31 mm will be prepared by a turning machine and then once it's ready hand laying of E-Glass Fiber/Epoxy will be done to reach the desired outer diameter and then vacuumed to have a stronger frame.
CNC Aluminum/Plywood	Medium	Centering rings will be cut as desired using CNC machine and then mounted into the inner tube using Araldite 2015. The two aluminum centering rings will have 3 cuts in them to insert the fins inside them. The boat tail will then be mounted at the back of the inner tube and centering ring as well using Araldite 2015.

The coupler will hold the two frames together (Primary and Main). The coupler will have one part attached by shear pins to the primary body while the other side will be inside the main body and mounted with M5 screws. Once the separation is activated for the release of the main parachute the piston separation system will push the coupler breaking the shear pins and separating the bodies (Primary and Main) from each other and releasing the main parachute.

Engine Section Mechanical View & Detail

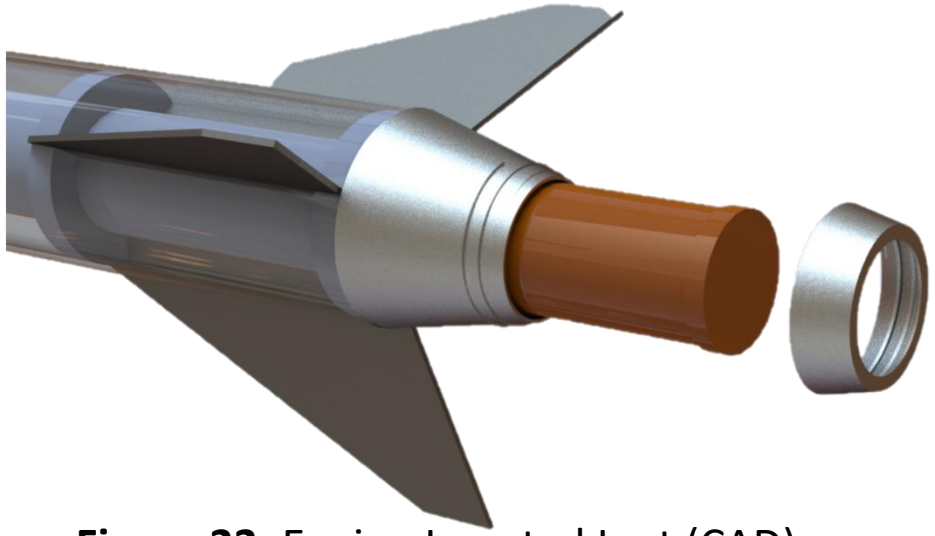

Figure 23. Engine Inserted Last (CAD).

As previously stated, the engine inner tube will be an E-fiber/Epoxy tube that will be made by hand lying on a male aluminum mold, and then vacuumed. The centering rings will be CNC-cut, and all of the pieces will be assembled as illustrated with Araldite 2015. The single-component will then be put into the main frame and secured to the engine block with eight M5 screws. The engine will be fitted as depicted in Figure 23 and followed by a rotating engine retainer after the complete rocket has been built.

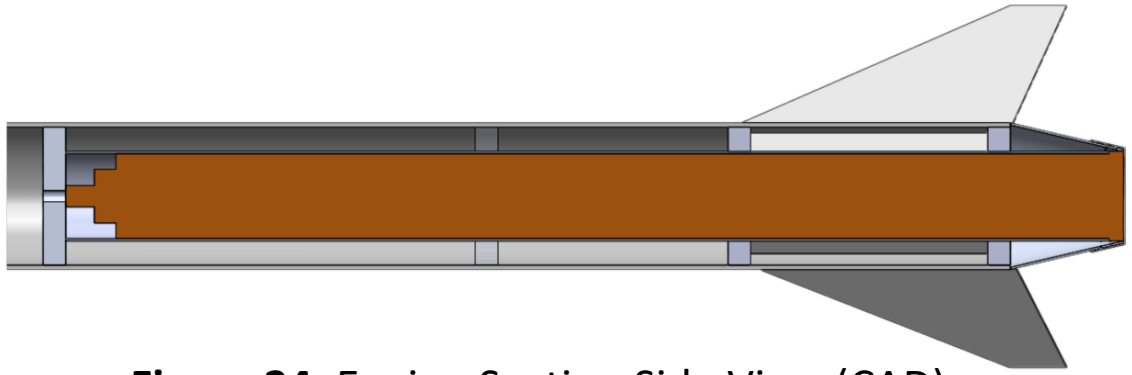

Figure 24. Engine Section Side View (CAD).

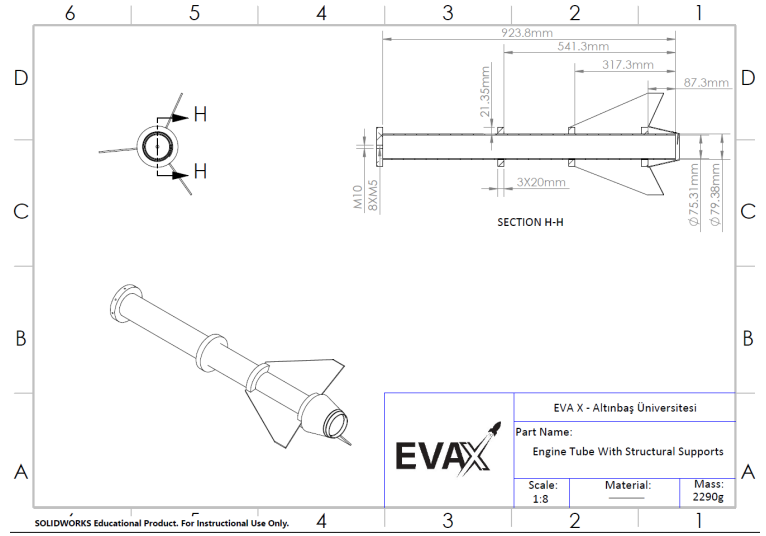

Figure 25. Engine Section Side View Technical Drawing.

Engine Section Mechanical View & Detail

The fins and boat tail will also be mounted into the aluminum centering rings made. A video has been attached showing the motor (in dark orange) being inserted last into the rocket.

Engine attachment video : https://youtu.be/X4Z-c_iVJyg

Rocket Assembly Strategy

Figure 25. Exploded CAD of the rocket.

Rocket Assembly Strategy

- The nose cone, primary frame, and main body are the three main components of the rocket. Two further elements will be included in the Main Frame: a coupler and a one-piece engine block part.
- To start, the Avionics bay will contain the separation systems inside of it, they will be put into the primary body and secured with four M5 screws. The Drogue parachute, which is linked to a 5 m shock chord, will then be placed into the primary body, with the shock chord end secured to the separation system's M10 eyebolt with a locking carabiner.
- After that, the payload and its parachute will be fitted into the frame, behind the Drogue Parachute. Afterward, the other end of the shock chord will be attached to the Nose Cone tips M10 eyebolt with a locking carabiner. The Nose Cone shoulder will then be screwed into the Primary body with three M3 nylon shear pins. The main parachute will then be secured to the opposite end of the separation system's M10 eyebolt using a locking carabiner, located on another 5 m shock cord, from the other end of the primary body.
- The one-piece engine block part is constructed of an inner tube that houses the motor and is encircled by three centering rings. The engine block ring will be fastened to one end of the inner tube, and the boat tail will be attached to the other. Two centering rings will have cuts in them for the three fins that will be installed.
- When the one-piece engine block part is ready, it will be put into one end of the main body, where cuts for the fins will be made. The coupler will be put in place with four M5 screws on the opposite end of the main body. After attaching the other end of the Main Parachute to the M10 attached to the Engine block, the main body will be ready to be put into the primary body, and three nylon shear pins will be screwed into the coupler and primary body to ensure that the two frames (Main and Primary) are securely attached.

Rocket Assembly Strategy

- Finally, a revolving engine retainer is used to hold the motor into the inner tube. The avionics bay will contain an extra space specifically for the Referee Altimeter.

We will not be using a hot gas generator for our separation instead we are using a CO_2/Piston system to activate our separations. Attached below is a video to further clarify our rocket assembly strategy.

Rocket assembly video: https://youtu.be/X4Z-c_iVJyg

Recovery System Mechanical Appearance

Figure 26. Parachute Opening System.

Figure 27. Parachute Section View,
Drogue and PAYLOAD Parachute Detailed CAD.

Figure 28. Parachute Section View,
Main Parachute Detailed (CAD).

Recovery System–Parachute Opening System

When it came to the separation system that would be employed, we weighed all of the choices before making a decision. When we looked at hot gas generators, it appeared like it would be too dangerous to do, and we'd be limited in our testing since we'd need a lot of gun powder. When we looked into mechanical spring systems, we found that they take too much weight and volume to in the rocket, despite the fact that testing would be considerably easier. Finally, we settled on a cold gas generators/Piston system, deciding that such a system would allow us to test without the risks of hot gas while also allowing us to rerun tests easily.

We have purchased two 25 mm diameter aluminum pistons that will provide a force of roughly 260 N, which will be enough to break the shear pins that are holding the nose cone and the main body to the primary body. Each system will be triggered using a servo motor and a tiny CO_2 inflator, as shown in Figure 28. When the servo motor receives a signal from our avionic computer, it will rotate, pushing the CO_2 inflator with a torque of 4.2 kgf.cm, which will release the compressed CO_2 into the piston, and push an Aluminum plate towards either the coupler or the nose cone shoulder with the stated force, breaking the nylon shear pins that hold the frames together. One piston has two servo motors and two CO_2 inflators linked to it; the other piston, on the other hand, travels through the avionics bay and is mounted on the interior. The servo motor wires also pass through to connect to the computers. The main parachute separation will be activated by the piston that travels through the avionics bay, while the drogue and PAYLOAD parachute separation will be activated by the piston that has the servo motors and CO_2 inflators. The separation system will take 448751.99 mm^3 of volume inside the rocket.

Recovery System–Parachute Opening System

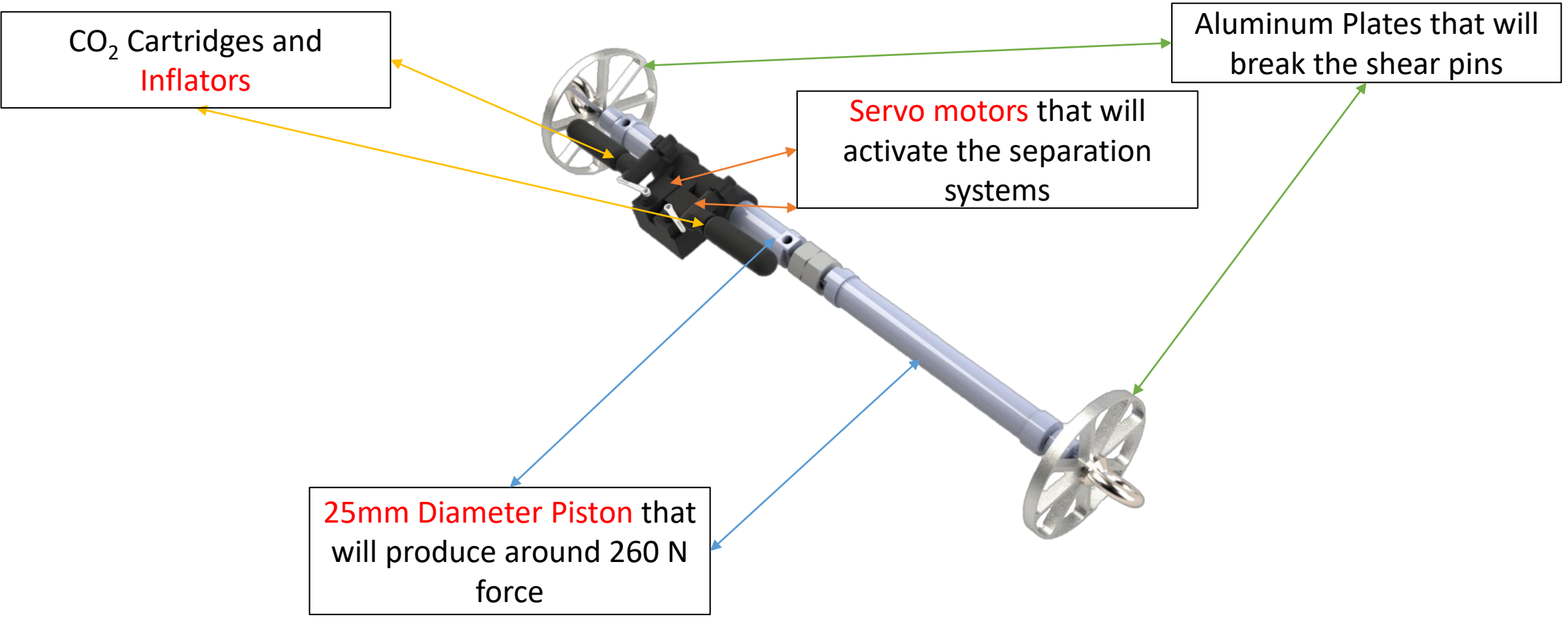

Figure 29. Parachute Opening System Detailed (CAD).

Recovery System–Parachute Opening System

Figure 30. 1st Recovery Phase Detailed (CAD).

Figure 31. 2nd Recovery Phase Detailed (CAD).

Once the rocket reaches apogee, the first recovery phase will begin. The avionics system will transmit a command to the appropriate servo motor, which will then push the CO_2 inflator, which will then force the payload into the nose cone shoulder, breaking the shear pins. The piston will not separate the rocket, but will also force the parachutes outside of it, kicking off the first phase of recovery.

The second phase of recovery will begin about 500 meters high. The avionics system will send a signal to the relevant servo motor to pressurize the CO_2 inflator and push it with the required force to break the shear pins attached to the coupler. As a result of the shock chord's descent, the main parachute is pushed outside the rocket, initiating the second recovery phase.

Hot Gas Generator Requirements

We will not be using a hot gas generator for our separation.

Recovery System–parachutes-one

Main Parachute (8 pieces) (R=270),

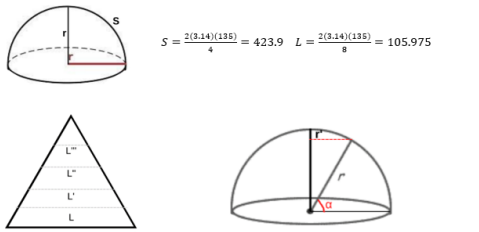

$S = \frac{2(3.14)(135)}{4} = 423.9 \quad L = \frac{2(3.14)(135)}{8} = 105.975$

Degree	rcos α=r'	2πr'	2πr'/8=L'
0	135	847.80	105.97
10	132.94	834.92	104.36
20	126.85	796.67	99.58
30	116.91	734.21	91.77
40	103.41	649.45	81.18
50	86.72	544.64	68.08
60	67.50	423.90	52.98
70	47.52	298.44	37.30
80	23.44	147.21	18.40
90	0.00	0.00	0.00

Payload Parachute (6 pieces) (R=110)

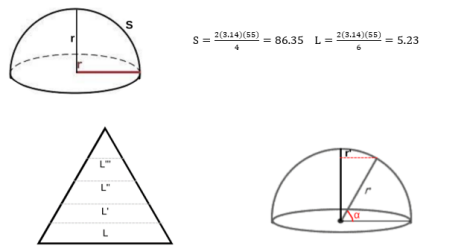

$S = \frac{2(3.14)(55)}{4} = 86.35 \quad L = \frac{2(3.14)(55)}{6} = 5.23$

Degree	rcos α=r'	2πr'	2πr'/6=L'
0	55.00	345.40	57.56
10	54.16	340.15	56.69
20	51.68	324.56	54.09
30	47.63	299.12	49.85
40	42.13	264.59	44.09
50	35.35	222.01	37.00
60	27.50	172.70	28.78
70	19.36	121.58	20.26
80	9.55	59.97	9.99
90	0.00	0.00	0.00

Drogue Parachute (12 pieces) (R=120),

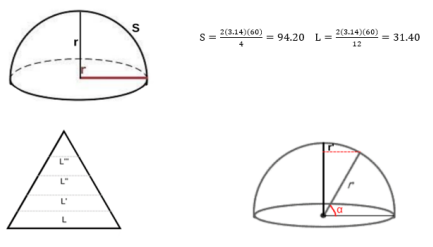

$S = \frac{2(3.14)(60)}{4} = 94.20 \quad L = \frac{2(3.14)(60)}{12} = 31.40$

Degree	rcosα=r'	2πr'	2πr'/12=L'
0	60.00	376.80	31.40
10	59.08	371.07	30.92
20	56.38	354.07	29.50
30	51.96	326.31	27.19
40	45.96	288.64	24.05
50	38.56	242.20	20.18
60	30.00	188.40	15.70
70	21.12	132.64	11.05
80	10.41	65.43	5.45
90	0.00	0.00	0.00

Sheet 1. Parachute Fabric Calculations Sheet.

The parachutes were designed in a hemispherical shape because it is the easiest to manufacture and calculate the fabric amount while maintaining the desired fall rates.

Because of its strong heat resistance and durability to bear flight forces while also being light, Ripstop Nylon was chosen as our parachute material. For the production of each of the parachutes, calculations were produced as illustrated in Sheet 1. The results of the calculations will be supplied to a tailor together with the amount of fabric required for manufacturing.

Table 13. Parachutes Features.

Parachute	Material	Color	Geometry	Mass (g)	Open Diameter (m)	Spill Hole Diameter (m)	Area (m^2)	Descent Velocity (m/s)
Drogue Parachute	40D Ripstop Nylon	Red	Hemispherical	115.00	1.20	0.24	1.0857	20.26
Main Parachute	40D Ripstop Nylon	Orange	Hemispherical	435.00	2.70	0.54	5.4965	8.57
PAYLOAD Parachute	40D Ripstop Nylon	Black	Hemispherical	70.40	1.10	0.22	0.9123	10.53

Recovery System–parachutes-2nd

Table 14. Parachutes Descent Calculations .

Parachute	Mass to carry (kg)	Air Density at Descend Altitude (kg/m³) [2]	Open Diameter (m)	Spill Hole Diameter (m)	Area (m²)	Calculated Descent Velocity (m/s)
Drogue Parachute	18.306	1.007	1.20	0.24	1.0857	20.26
Main Parachute	18.306	1.112	2.70	0.54	5.4965	8.57
PAYLOAD Parachute	4.158	1.007	1.10	0.22	0.9123	10.53

Using the velocity during recovery equation (2) [1] the descent velocity was calculated and recorded in Table 14. Where W is the weight to be carried by the parachute in kg, C_d is the coefficient of drag, ρ is the air density at descending altitude in kg/m³, and A is the area of the parachute in m².

$$V = \sqrt{\frac{2W}{C_d \rho A}} \quad (2)\ [1]$$

Recovery System–parachutes-3rd

Rocket Recovery Process

Table 15. Rocket Recovery Components.

Copmonent	Role in the Recovery Mission
Grove - GPS (Air530) Module GY-NEO 8M GPS Module	Data of altitude, latitude and longitude information needed for recovery.
LoRa SX1278 Telemetry Module DRF7020D27 Telemetry Module	Transfer of data from GPS modules to ground station.
433 MHZ TX433-JKD-20P Antenna	Ensuring the operation of telemetry modules
5V Buzzer	Assisting with sound

During the rescue, the main avionics and backup avionics GPS modules, which play an active role in the rocket, will transmit altitude, latitude, and longitude data to the ground station with a 5 MHz frequency by LoRa SX1278 and DRF7020D27 telemetry modules, in line with ANNEX-8 requirements. The data will be transferred to the ground station on the 433 MHz band and with the data packaging on page 38. A 433 MHz TX433-JKD-20P antenna will be used for the telemetry modules to work. 5V Buzzer will be used to assist with sound during recovery.

Payload Recovery Process

Table 16. PAYLOAD Recovery Components.

Copmonent	Role in the Recovery Mission
Grove - GPS (Air 530) Module	Data of altitude, latitude and longitude information needed for recovery
LoRa SX1278 Telemetry Module	Transfer of data from GPS modules to ground station
433 MHZ TX433-JKD-20P Antenna	Ensuring the operation of telemetry modules

The Grove - GPS (Air530) GPS module, which is in the payload and plays an active role during the rescue, will transfer altitude, latitude, and longitude data to the ground station with a 5 MHz frequency the LoRa SX1278 telemetry module in line with the ANNEX-8 requirements. The data will be transferred to the ground station on the 433 MHz band and with the data packaging on page 28. A 433 MHz TX433-JKD-20P antenna will be used for the telemetry modules to work.

PayLoad

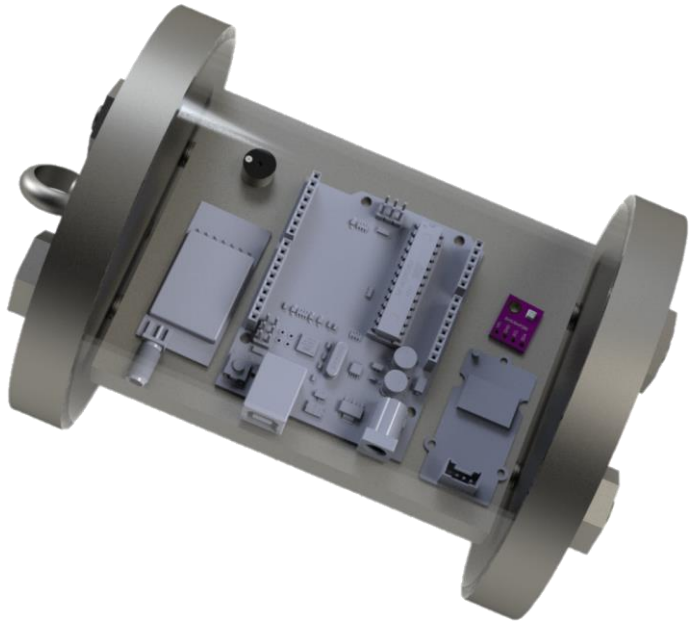

Figure 32. PAYLOAD 3D View (CAD).

The PAYLOAD will have a hole in the plexiglass through which a rotating switch will be linked to turn it on; the switch will then be connected to another switch located on the rocket's surface, allowing the payload to be turned on from the outside. As the first recovery phase begins at apogee, the piston system will get a signal from the avionics to push the PAYLOAD against the nose cone shoulder, breaking the shear pins, and pushing the PAYLOAD outside the rocket with its parachute. The PAYLOAD will be roughly 4158 g in weight.

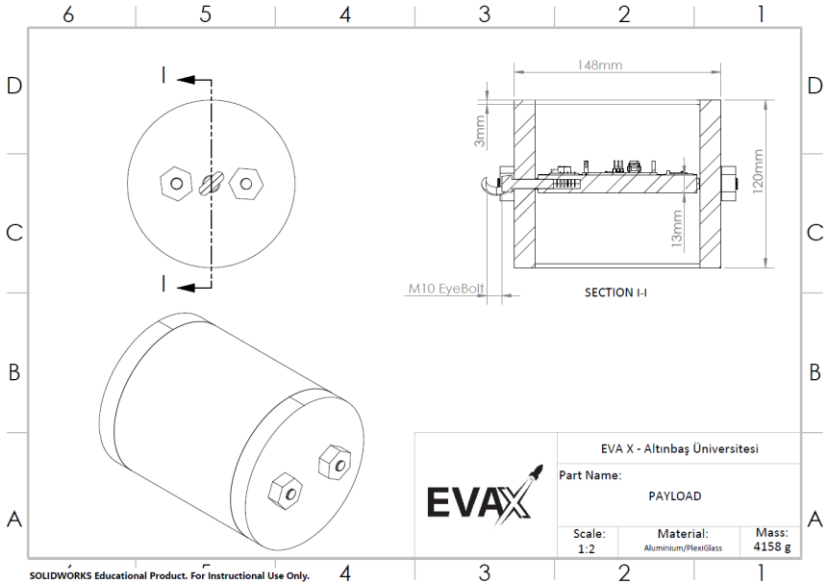

Figure 33. Payload Technical Drawing.

PayLoad

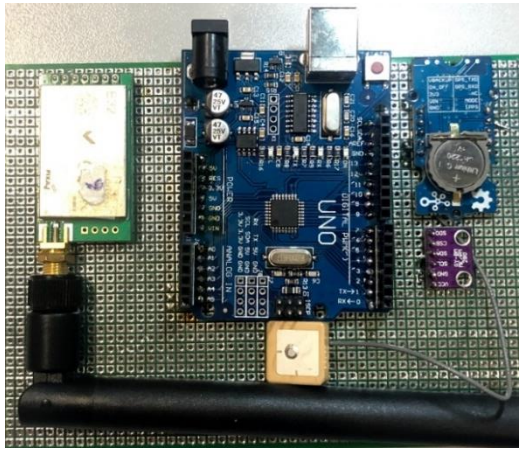

Figure 34. PAYLOAD Avionics.

Table 17. PAYLOAD Components .

Component	Product Name/Code	Purpose of Duty Payload Recovery
Processor	ATmega328PU Processor	Giving the necessary commands to the sensors and processing the data.
Pressure sensor	BME280 Pressure Sensor	Calculation of pressure, temperature and humidity data.
Communication Module	LoRa SX 1278 Telemetry Module	Enabling the transmission of data from the GPS module to the ground station.
GPS module	Grove - GPS (Air530) GPS Module	Sending the necessary data for the recovery process to the ground station with the help of the telemetry module.
Battery	GP GP1604AU Alkaline Battery	Ensuring that the necessary power is supplied to the system.
Antenna	TX433-JKD-20P 433 MHz	Getting the telemetry module working.

The payload will transmit the BME280 sensor pressure, temperature, and humidity data, and the Grove - GPS (Air530) module ANNEX-8 requirements of altitude, latitude, and longitude data via telemetry to the ground station with a frequency of 5 Mhz. LoRa SX 1278 telemetry module and TX433-JKD-20P antenna operating in the 433 MHz band were selected for data transmission. Data packet <PACKAGE NUMBER>;<TEAM ID>;<GPS ALTITUDE>;<GPS LATITUDE>;<GPS LONGITUDE>;<PRESSURE>;<TEMP>;<HUMIDITY> will be in the form. The data received by the LoRa SX1278 in the ground station will be sent to the computer with the Arduino Nano. The data will be displayed on the screen with the application designed by EVA X, Figure 56 on slide 61 .and location data will be obtained for recovery. The data on the computer will be transferred to the RGS device with the packaging in accordance with the ANNEX-8 requirements and the data will be transmitted to the referee ground station.

Recovery System Prototype Test

In the shared test calendar, green boxes indicate the tests that will be completed during the CDR phase. All tests will be held at Altinbas University Mahmutbey Campus.

Table 18. Schedule of Recovery System Tests.

	2022			
	May 1st	May 6th	May 8th	May 11th
Prototype Manufacturing				
Parachute Opening Test				
Separation Activation Test				
CO2 Recovery System Test				
Parachutes Strength Test				
Shock Chord Strength Test				

Recovery System Prototype Test

As for the recovery system prototype tests, a prototype nose cone and frame are being prepared and will be ready on the 6th of May for testing. Once the protypes are ready a video will be shot from the 6th to 11th of May.

- Prototype level assembly and setup stages of the recovery system and functionality tests:

In the video it will show how the separation system will be assembled into the primary frame with the parachutes and shock chord and a test of the first and second recovery phase will be done showing the nose cone and coupler being separated from the primary frame thanks to the CO_2 Piston system force that will break the nylon shear pins and releasing the parachute outside. Success in this test will show that the parachutes will be released out of the rocket and will be functional for recovery and that the separation will be also be successful.

- Parachutes Opening/Functionality Tests:

The parachutes opening tests will also be done by releasing the folded parachutes out a moving car and held to check if the parachutes would open once released out the rocket. Also, another test will be done were around 4 kgs of weight will be attached to the parachutes and released from a certain height showing it can handle descent forces. Once these tests are done and finished it will proof the functionality of our systems.

Tests will be uploaded on YouTube on our channel and also uploaded into the system before the 12th of May Deadline:
Recovery Prototype Test: [Recovery Prototype Test YouTube link will be placed here]

Analyzes

Structural/Mechanical Strength Analyses and Computational Fluid Dynamics Analysis were both performed using ANSYS 2020 R1. First, as shown in Figures 35 and 36, a mesh was created for the complete rocket as well as the nose cone. These meshes were created using a specific body scaling technique in which the element size was reduced near our body. Our boundary conditions have now been specified as a velocity intake and a pressure outlet, with walls on the other sides. We created an inflated section surrounding the body, with sizes calculated based on the Y+ value of 100.

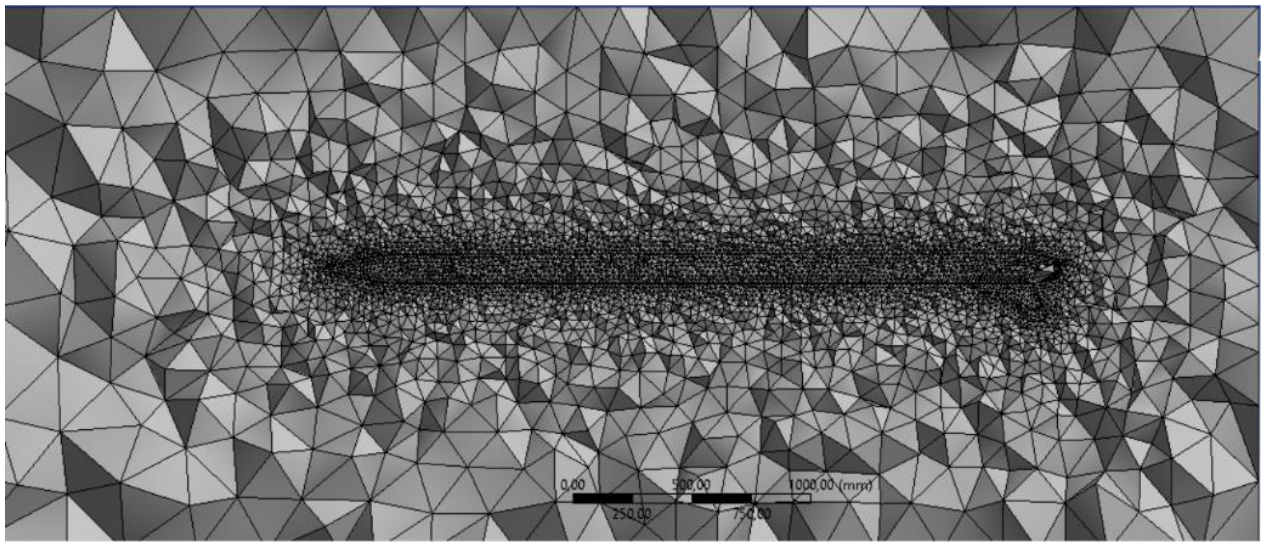

Figure 35. Mesh of Entire rocket.

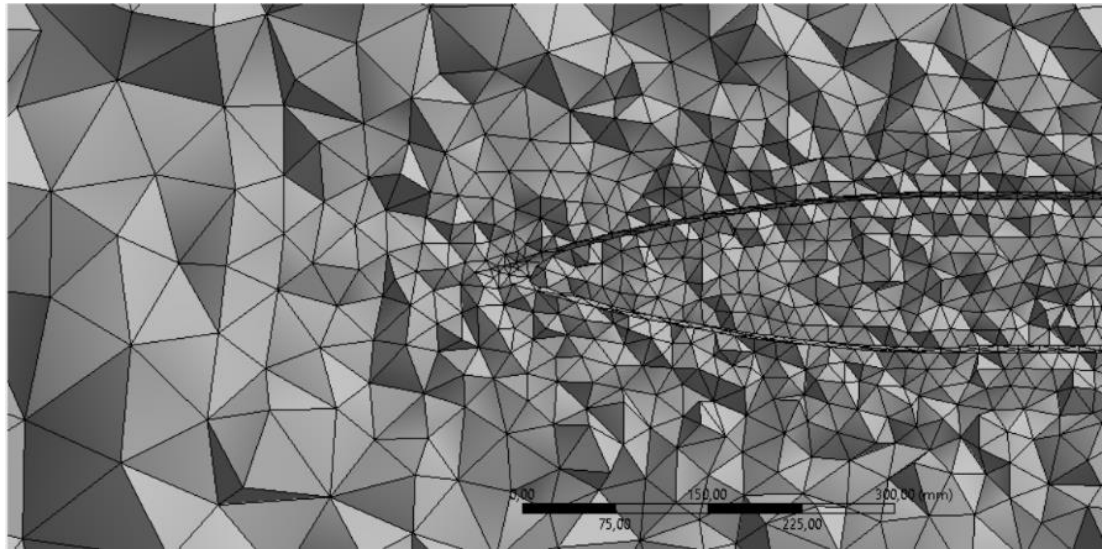

Figure 36. Mesh of Nose cone.

Analyzes

For the structural/Mechanical strength Analyses, the CAD drawing of our rocket has been uploaded into ANSYS and materials decided earlier in the reports were assigned. We applied some boundary conditions such as pressure effect at 3000-meter altitude as 0,07 MPa and drag force which affects directly the front section area on X-axis.

The results demonstrate that our rocket, which is made up of 70% E-glass fiber and 30% Aluminum 7075-T6, has enough durability at 3000-meter Altitude. On the engine block side, deformation was measured in fin plates, and stress was measured in the engine block. For our rocket design, these values are acceptable.

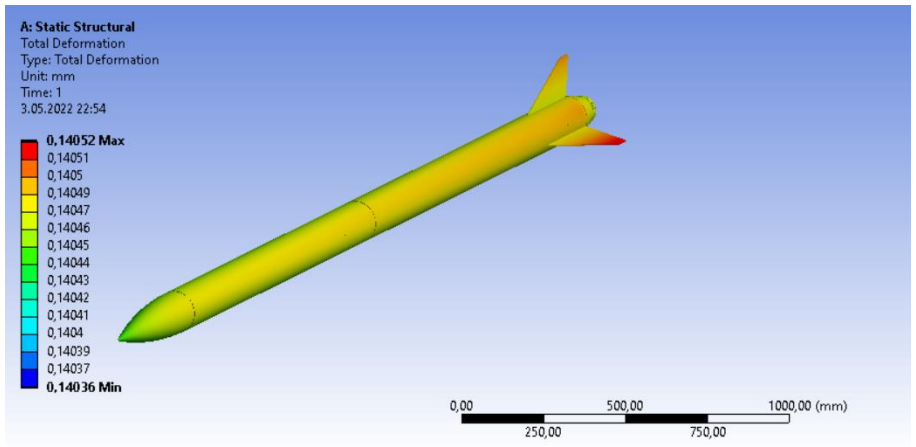

Figure 37. Total Deformation on Rocket.

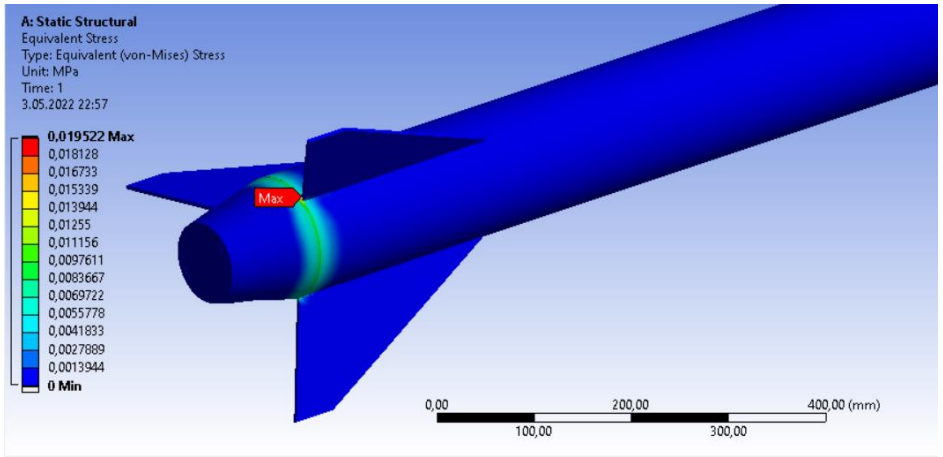

Figure 38. Equivalent Stress acting on the Rocket.

Analyzes

We used velocity inlet boundary conditions on the Z-axis for the nose cone. We utilized SST-k omega as a viscosity model and 280 m/s as an inlet value, both of which were supplied through open rocket simulation. Because the rocket is the interval in the atmosphere, we chose 1 atm as a pressure exit. We choose 1.007 kg/m^3 as a reference number since it is the density at apogee, and the front sectional area is 0.03 m^2 as computed from the SOLIDWORKS CAD model. We employed pressure velocity as a solution approach, with the solar gradient determined using the least-squares method and the pressure and momentum gradients chosen in the second order. This case is iterated 500 times and is taken as one state of the flight.

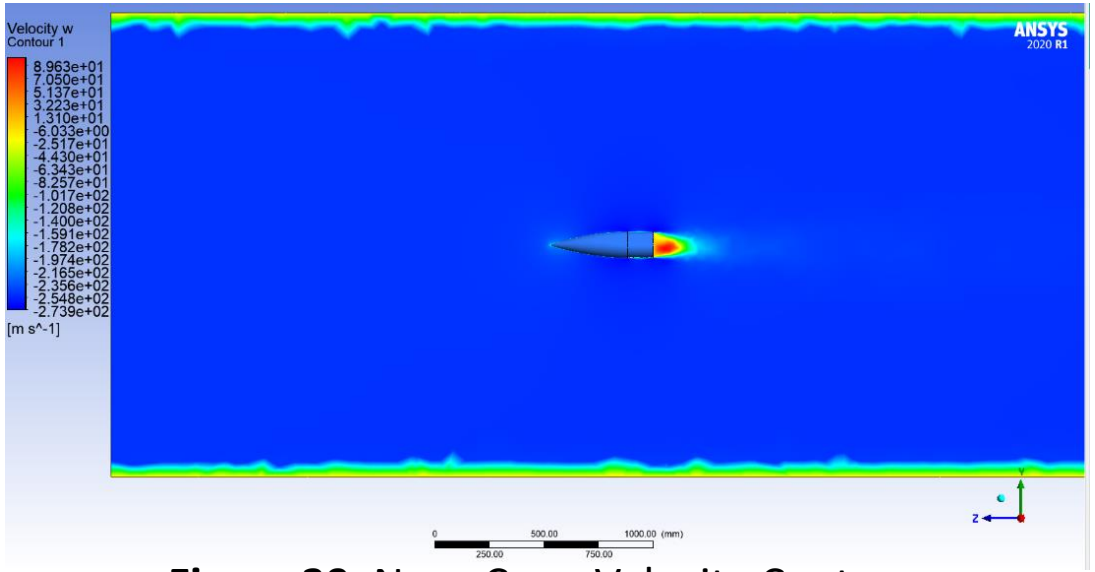

Figure 39. Nose Cone Velocity Contour.

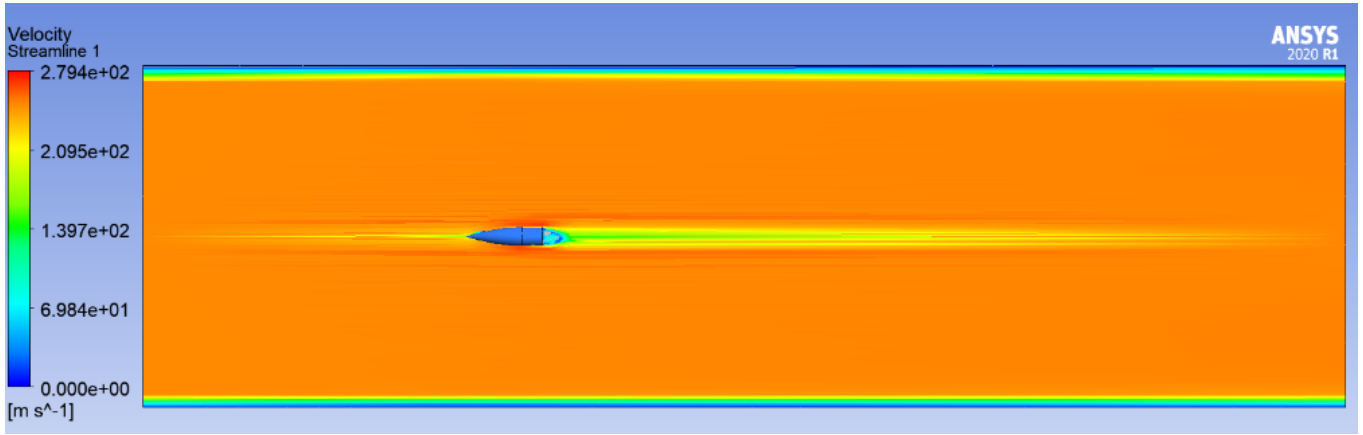

Figure 40. Nose Cone Velocity Streamline.

Analyzes

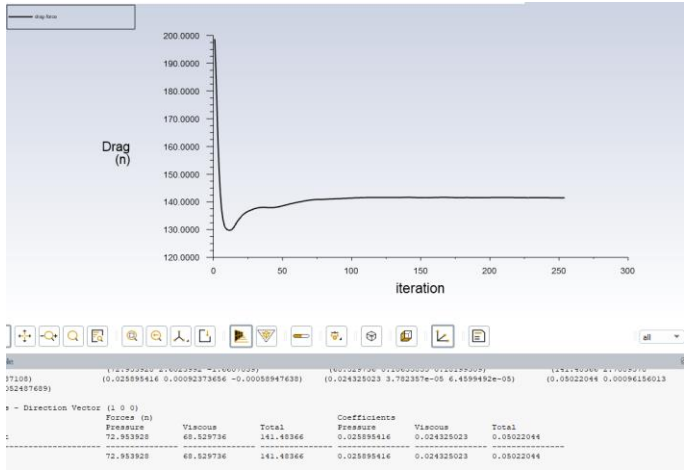

Figure 41. Drag Force Results.

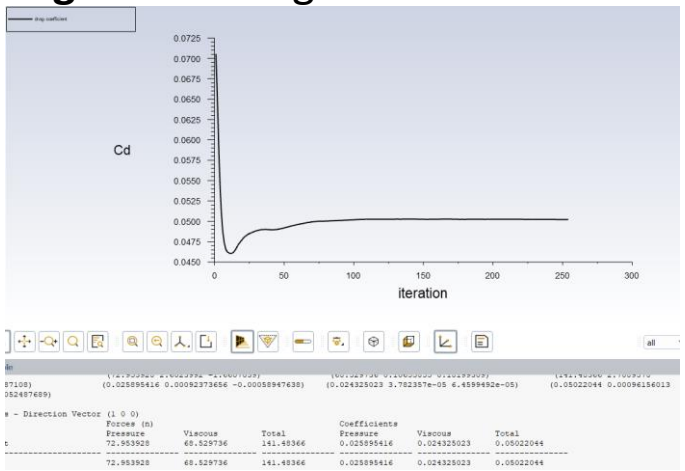

Figure 42. Coefficient of Drag Results.

The values of the tests were determined to be roughly 140 N of drag force with a drag coefficient of 0.05. For our design and flight, the values are deemed acceptable. The flow around the rocket at the backend is where the least velocity occurs, which is seen in the velocity contour. For the pressure contour, it can be observed that our rocket's 1 atm is sufficient to manage flight pressures, with the majority of pressures occurring at the rocket tips.

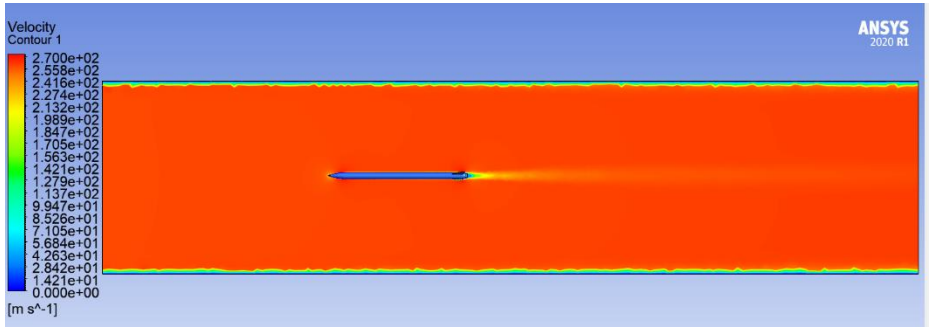

Figure 43. Rocket Velocity Contour.

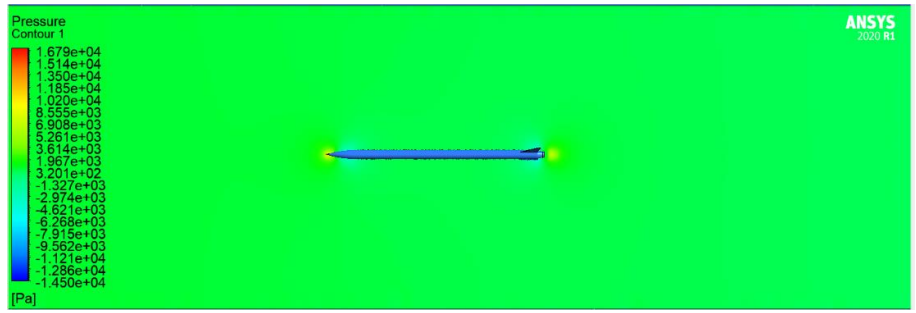

Figure 44. Rocket Pressure Contour.

Avionics– Summary

Avionic computers are originally designed by us. Table 18 shows the components of each system used in our avionics.

Table 18. Main and Backup Avionics Comparison.

Main Avionics System Parts and Codes	Purpose	Backup Avionics System Parts and Codes	Purpose	Differences	Similarity
ATmega2560 Processor	Processing and application of data.	ATmega2560 Processor	Processing and application of data.	-	The processors used are the same.
MPU6050 IMU Sensor	Acceleration and axis measurement.	BMP180 Pressure Sensor	Pressure, temperature and humidity measurement.	One is for acceleration and the other is for pressure.	It's used for the same goal of activating separation.
BME 280 Pressure Sensor	Pressure, temperature and humidity measurement.	BME 280 Pressure Sensor	Pressure, temperature and humidity measurement.	-	The purposes of the pressure sensors are the same.
LoRaSX 1278 Telemetry Module	Data transmission to ground station.	DRF7020D27 Telemetry Module	Data transmission to ground station.	Data transmission distances are different.	It's used for the same goal of data receiving.
Grove-GPS (Air530)	Making a position measurement.	GY-NEO 8M GPS	Making a position measurement.	Different sensitivity of dBm.	It's used for the same goal of ground recovery.
5V Buzzer	Helping to recovery.	5V Buzzer	Helping to recovery.	-	The Buzzers used are the same.
GP GP1604AU Alkaline Battery	Powering the system.	GP GP1604AU Alkaline Battery	Powering the system.	-	The batteries used are the same.
TX433-JKD-20P Antenna	Telemetry communication.	TX433-JKD-20P Antenna	Telemetry communication.	-	The antennas used are the same.

Avionics– Summary

The MPU6050 IMU sensor and BME280 pressure sensor will be used by the main avionics computer to trigger the servo motors linked to the 9th and 10th pins of the main avionics' computer, which will execute the separation procedures. The backup avionics computer's BMP180 and BME280 pressure sensors will be in charge of activating the servo motors attached to the backup avionics computer's 9th and 10th pins and executing the backup separation procedure if the main computer fails. Because there will be no electrical or cable connection between the two avionic computers, the backup avionic computer will perform the first and second separations at a 5-second delay from the main computer, that is, if there is no deviation in the data of the backup avionics BME280 pressure sensor and the BMP180 pressure sensor within the specified 5-second period, it will determine that the main avionic computer has failed to start the separation. If the backup avionic computer detects a variation in the sensor data within the 5-second time frame, it will cancel its own separation process and the servo motor will not execute the separation process, allowing the main avionics computers to complete the separation procedures without issue.

Figure 45. Avionics Bay 3D View (CAD).

Avionics – 1.System Detail/1

Table 19.1. Recovery Roles of Main Avionics Components.

Component	Product Name / Code / Type	Is Data Used in Recovery Algorithm?	The Function of the Data Used in the Recovery Algorithm
Processor	ATmega2560 Processor	(It will be left blank for the processor)	-
IMU Sensor	MPU6050 IMU Sensor	Yes	According to the acceleration data for the Y axis, the acceleration value after the previous acceleration value will be subtracted, and the minimum acceleration in the Y axis will be determined and the necessary condition for the first separation will be met.
Pressure Sensor	BME280 Pressure Sensor	Yes	In the incoming data, the pressure value after the previous pressure value will be subtracted and the separation will be performed according to the sign of the result. For the second separation, separation will be carried out according to the pressure value at 500 meters altitude, which was calculated beforehand.

Avionics – 1.System Detail/1

Table 19.2. Recovery Roles of Main Avionics Components.

Component	Product Name / Code / Type	Is Data Used in Recovery Algorithm?	The Function of the Data Used in the Recovery Algorithm
Communication Module	LoRa SX 1278 Telemetry Module	No	-
GPS Module	Grove - GPS (Air530) GPS Module	No	-
Buzzer	5V Buzzer	No	-
Battery	GP GP1604AU Alkaline Battery	No	-
Antenna	TX433-JKD-20P 433 MHz Antenna	No	-

Avionics – 1.System Detail/2nd

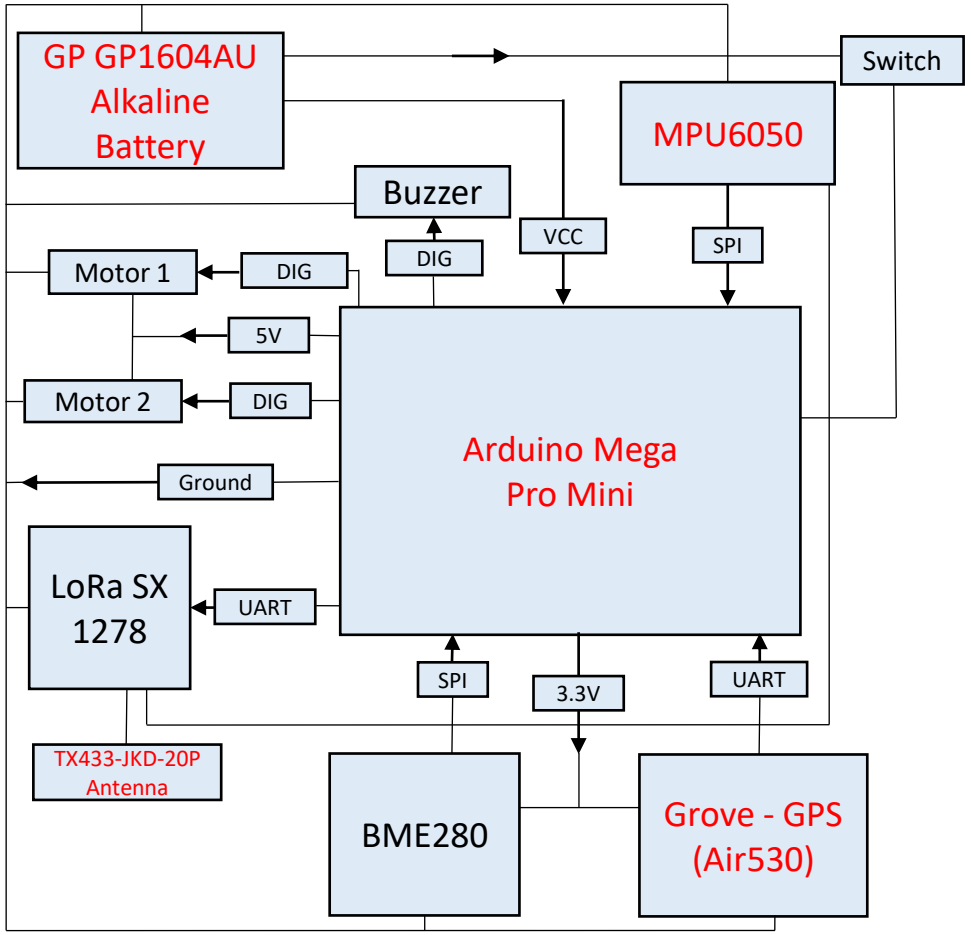

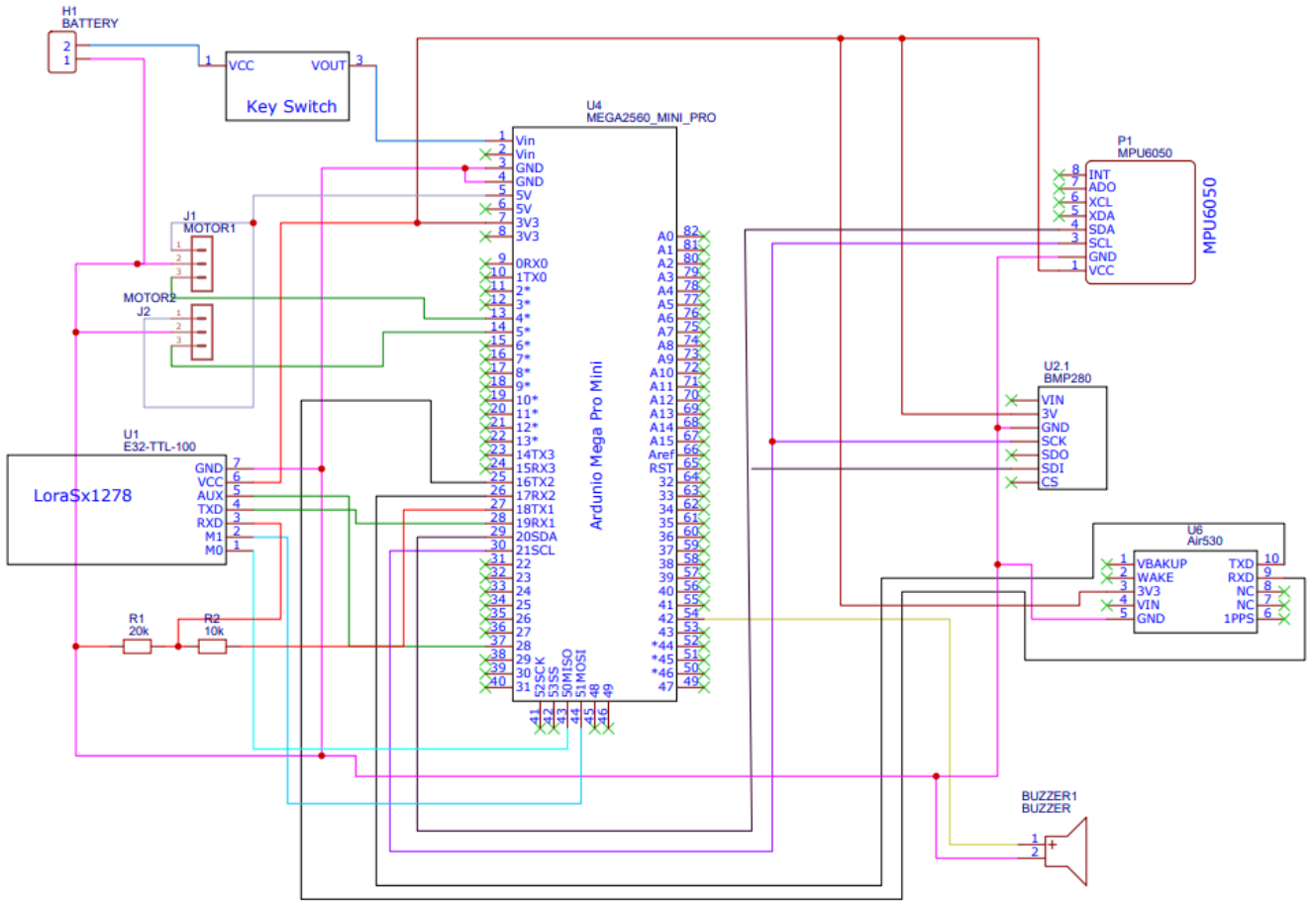

Figure 45. Main Avionics Block Diagram and Schematic.

Avionics – 1.System Detail/2nd

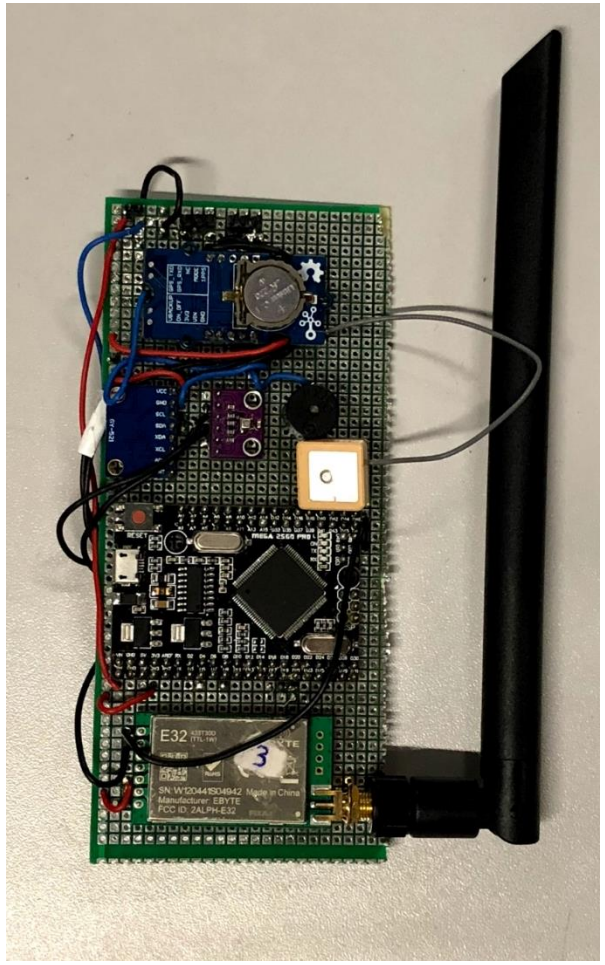

Figure 46. Main Avionics Photo.

We started with the main avionics system's first schematic design. Due to various defects in the PCB when produced, the PCB designs were drawn and soldered on the perforated plate instead. Main avionic board with 1 battery input, 2 servo inputs, Arduino Mega Pro Mini with Atmega2560 CPU, MPU6050 IMU sensor, BME80 pressure sensor, LoRa SX1278 telemetry module, Grove GPS (Air530), and Buzzer are all soldered in a specific order on a perforated plate. Later, the perforated plate's short-circuited section was utilized as a power distribution block, and power connections were built using soldering to ensure that the data link between the Arduino Mega Pro Mini and the sensors was maintained. PCB cutting will later be made to replace the perforated plate. Additional connectors for servo motors and the GP GP1604AU Alkaline Battery are added, which is only used in the main avionics as each computer will have its own battery. Finally, the main avionics system is up and running.

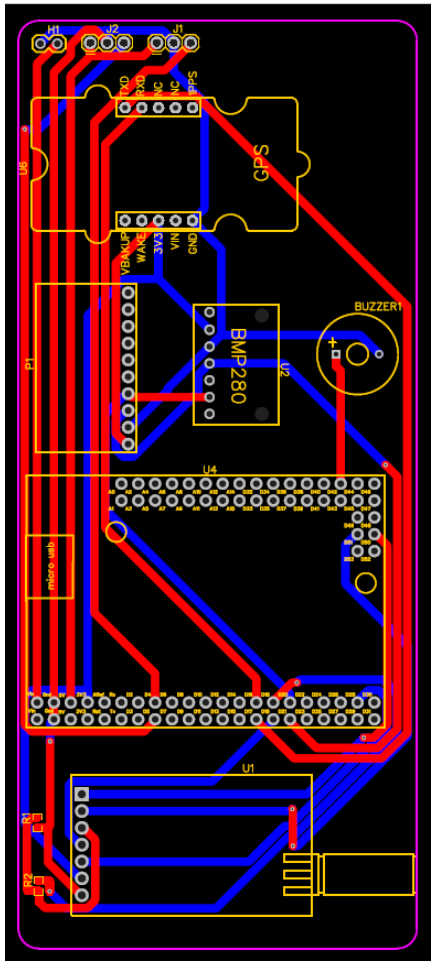

Figure 47. Main Avionics PCB Design.

Avionics – 1.System Detail/3

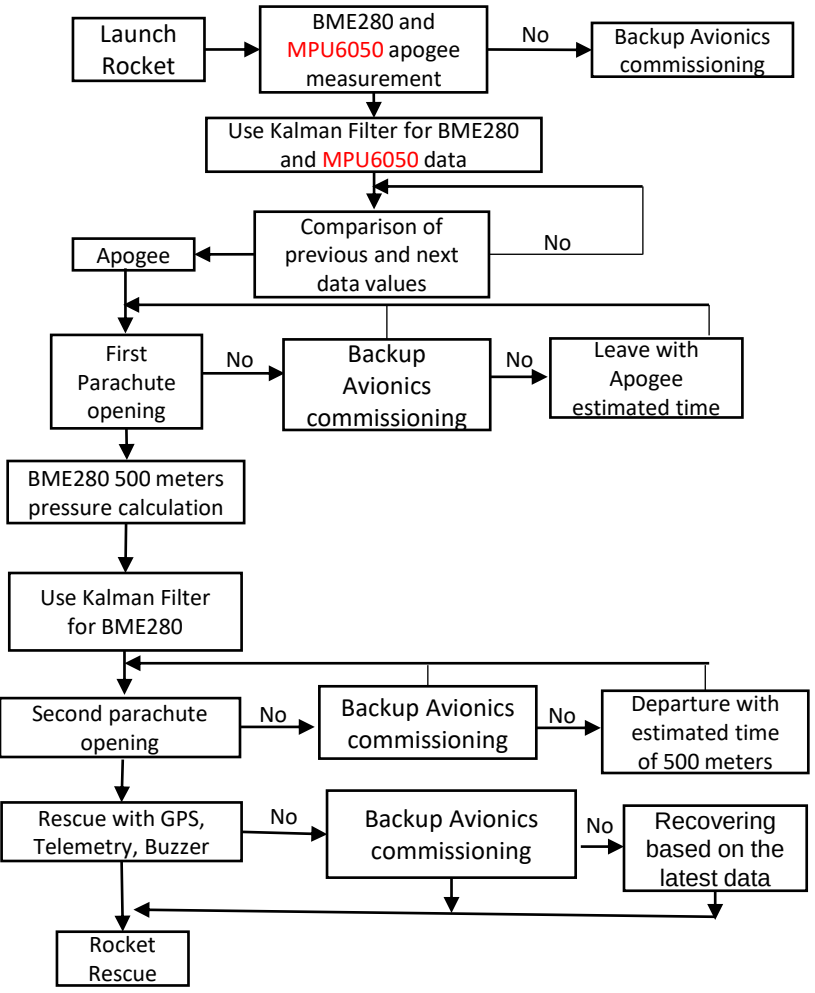

Figure 48. Main Avionics Algorithm.

When the rocket reaches the apogee point, the BME280 pressure sensor will compare the next data to the previous one and determine whether the pressure has decreased. When the lowest point on the Y-axis acceleration is reached, the MPU6050 IMU sensor will recognize that it has reached its peak. Once both conditions are met the first parachute will be opened. Otherwise, separation will be done according to the apogee departure time that has been pre-calculated. The BME280 pressure sensor will calculate an altitude value based on the pressure at a predefined distance of roughly 500 meters for the rocket's second parachute, once that calculated value is defined the rocket to separation will activate. When the rocket lands and the recovery procedure starts, the Grove GPS (Air530) will broadcast position data to the LoRa SX1278 telemetry module to allow us to locate it The buzzer will be used to assist during the recovery process. All data that will trigger the separation will be ran through Kalman Filter.

Table 20. Separation Activation Parameters List (Main).

Parameters to Trigger the System	Reason of Choosing	Sensors from Which Data is Received
Pressure	Pressure can accurately reflect the altitude of the rocket as they are proportional.	BME280 Pressure Sensor
Y-axis Acceleration	Y-axis acceleration is zero at the apogee.	MPU6050 IMU Sensor
Calculated Time From Simulation	To be used as a last resort in the event of a possible inability to leave.	Arduino Mega Pro Mini Function

Avionics – 1.System Detail/3

Data filtering is a mathematical algorithm for predicting the next data by modeling data when the data read is uncertain. The main avionics uses the Kalman Filter. The Kalman Filter, by including certain noises, provides more precise data after mathematical operations are done. The data from the BME280 sensor and the MPU6050 sensor is processed using the Kalman Filter. The BME280 sensor measures the data in real-time and provides the system with real-time pressure data. The data is put through the Kalman filter and precise data is generated and used instead because the incoming data is fluctuating, and not exactly near to reality. The MPU6050 sensor returns data values into the system by calculating instantaneous acceleration changes. Since the data constantly takes different values under different conditions, sharper values are obtained and used bypassing the data from the sensor through the Kalman filter as well.

Kalman Filter Formulization

Formula : $\bar{x}_K = K_K.Z_K + (1-K_K).\bar{x}_{K-1}$ (3)[4].

The formula (3) contains the estimated value of the X value, $\bar{x}_K$. The Z_K value is the measured value and does not give the correct output before filtering. K_K is the Kalman gain value multiplied by the measured value. $\bar{x}_{K-1}$ is the estimated value of X in its previous state and is multiplied by $(1-K_K)$.

After the actual values of the main avionics' computer sensors are found with the Kalman filter formula, their data is used for separation.

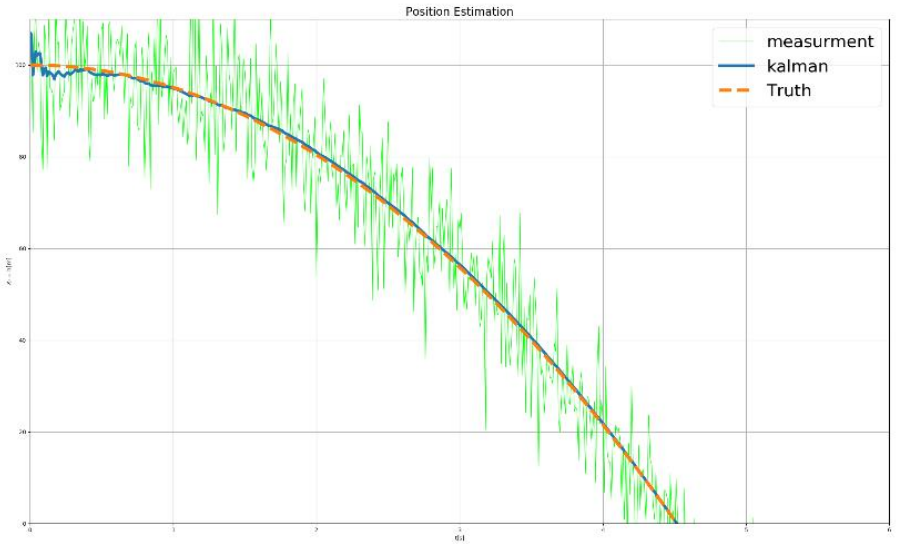

Figure 49. Kalman Filtered Output Chart Example [5].

Avionics – 2.System Detail/1

Table 21.1. Recovery Roles of Backup Avionics Components.

Component	Product Name / Code / Type	Is Data Used in Recovery Algorithm?	The Function of the Data Used in the Recovery Algorithm
Processor	ATmega2560 Processor	(It will be left blank for the processor)	
Pressure Sensor	BMP 180 Pressure Sensor	Yes	Signal status will be determined by subtracting the previous data from the next data in the calculated pressure values, and the first separation will take place when it is sense that the apogee point has been reached. The second separation will take place using a predetermined 500 meters altitude pressure.
Pressure Sensor	BME280 Pressure Sensor	Yes	Received data will be calculated from the previous pressure value difference and separated according to the sign of the result. In the second separation, it will be separated according to the pressure value at 500 meters previously calculated.

Avionics – 2.System Detail/1

Table 21.2. Recovery Roles of Backup Avionics Components.

Component	Product Name / Code / Type	Is Data Used in Recovery Algorithm?	The Function of the Data Used in the Recovery Algorithm
Communication Module	DRF7020D27 Telemetry Module	No	-
GPS Module	GY-NEO 8M GPS Module	No	-
Buzzer	5V Buzzer	No	-
Battery	GP GP1604AU Alkaline Battery	No	-
Antenna	TX433-JKD-20P 433 MHz Antenna	No	-

Avionics – 2.System Detail/2

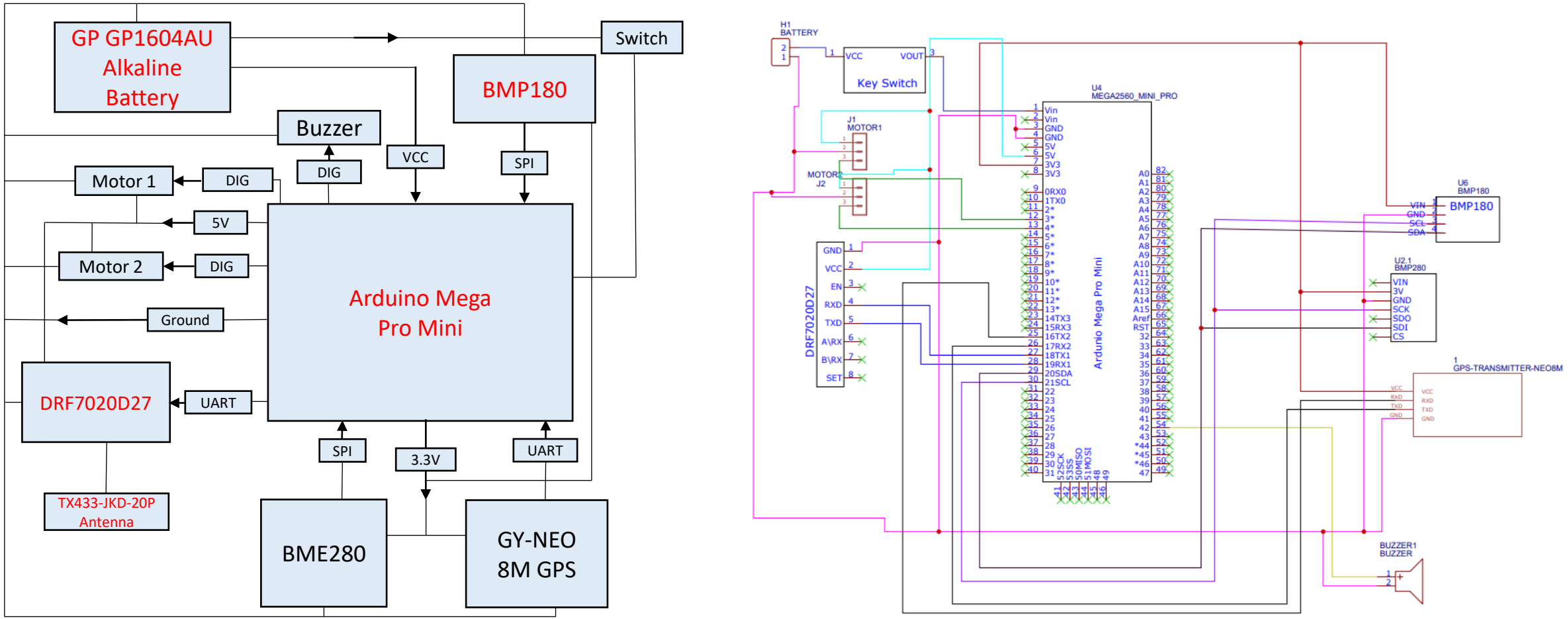

Figure 50. Backup Avionics Block Diagram and Schematic.

Avionics – 2.System Detail/2

Figure 51. Backup Avionics Photo.

We started with the backup avionics system's first schematic sketch. The soldering of the cable connections between the sensors was then completed on the perforated plate. A perforated plate has been soldered with a backup avionics board, 1 battery input, 2 servo inputs, Ardunio Mega Pro Mini with Atmega2560 CPU, BME280 pressure sensor, BMP180 pressure sensor, DRF7020D27 telemetry sensor, GY-NEO 8M GPS, and Buzzer. The sensors were powered by the short-circuited portion, which also served as a power distribution system. The Arduino Mega Pro Mini was then soldered for features such as a signal exchange. Additional connectors for servo motors have been added, as well as a GP GP1604AU Alkaline Battery for the backup computer. As a result, the backup avionics system is ready for operation.

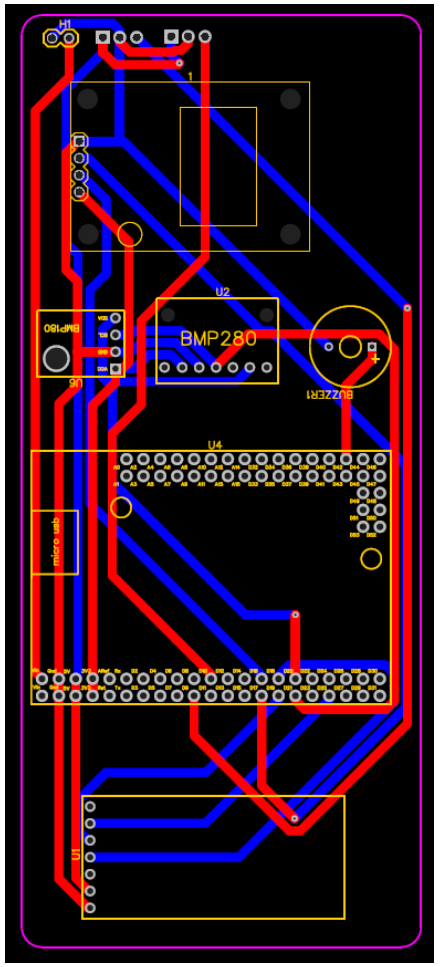

Figure 52. Backup Computer PCB.

Avionics – 2.System Detail/3

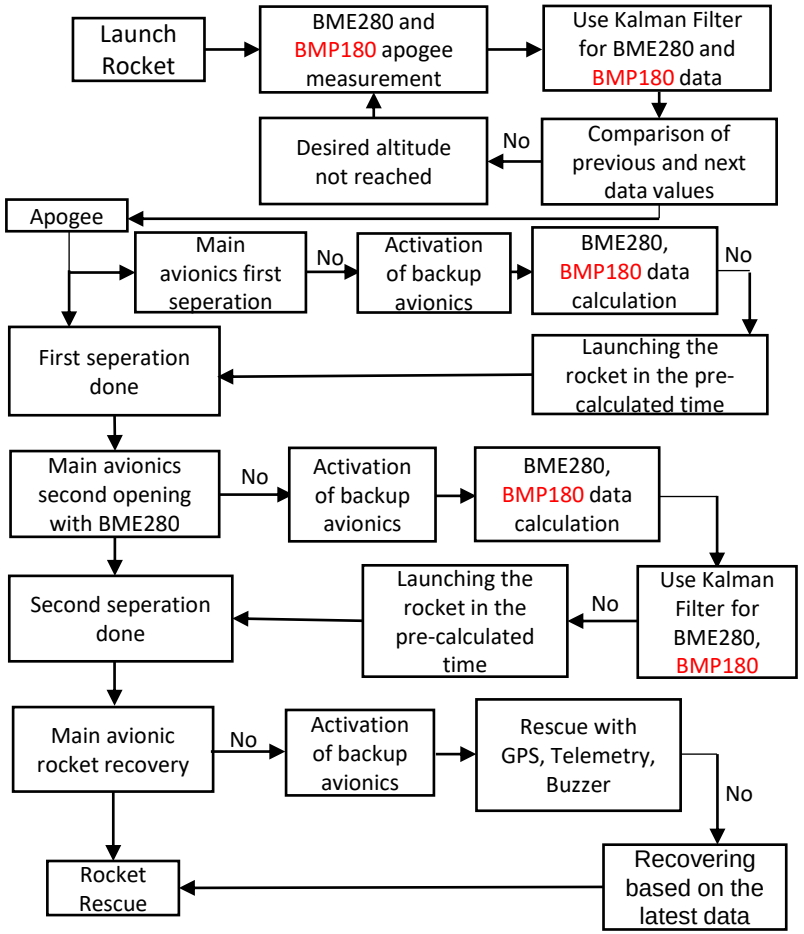

Figure 48. Backup Avionics Algorithm.

By subtracting the data from the prior data, the BME280 and BMP180 sensors will identify if the pressure is dropping once the rocket reaches the apogee point. The backup computer will start 5 seconds after the main computer fails to produce separation at the apogee point, hence starting the separation. Otherwise, separation will be done according to the apogee departure time that has been pre-calculated. The BME280 and BMP180 sensors will allow the rocket to open according to the pressure at a predefined distance of around 500 meters if the main computer is unable to complete the second parachute opening. Finally, If the main avionics fail to deliver data for recovery after the rocket has landed, the DRF7020D27 telemetry module will receive location data from the GY-NEO 8M GPS and the recovery procedure will start. During the recovery phase, the buzzer will be used to help. All data that will activate separation will be ran through Kalman Filter.

Table 22. Separation Activation Parameters List (Backup).

Parameters to Trigger the System	Reason of Choosing	Sensors from Which Data is Received
Pressure	Pressure can reflect the altitude of the rocket as they are proportional.	BME280, BMP180 Pressure Sensor
Pressure	Using a second pressure sensor gives our data more reliability	BME280, BMP180 Pressure Sensor
Calculated Time From Simulation	To be used as a last resort in the event of a possible inability to leave.	Arduino Mega Pro Mini Function

Avionics – 2.System Detail/3

Data filtering is a mathematical algorithm for predicting the next data by modeling data when the data is uncertain. The Kalman Filter basically includes certain noises, allowing us to obtain sharper and more precise data after mathematical operations. The spare avionics computer uses the Kalman Filter. Kalman Filtration is used in the BME280 pressure sensor and the BMP180 pressure sensor. BME280 pressure sensor and BMP180 pressure sensor work in similar logic as filtering. In pressure sensors, the data is measured instantly and gives instant pressure data to the system. Since the pressure data obtained varies and can be far from realistic, the data is passed through the Kalman Filter and precise results are obtained.

Kalman Filter Formulization

Formula: $\bar{x}_K = K_K.ZK + (1-K_K).\bar{x}_{K-1}$ [4] (3).

Formula (3) contains the predictive value of X value, $\bar{x}_K$. The Z_K value is the measured value and does not give the correct value before filtering. K_K is the Kalman gain value multiplied by the measured value. $\bar{x}_{K-1}$ is the estimated value of X in its previous state and is multiplied by $(1-K_K)$. After calculating the actual values of the redundant avionics' computer sensors with the Kalman filter formula, their data is used for separation.

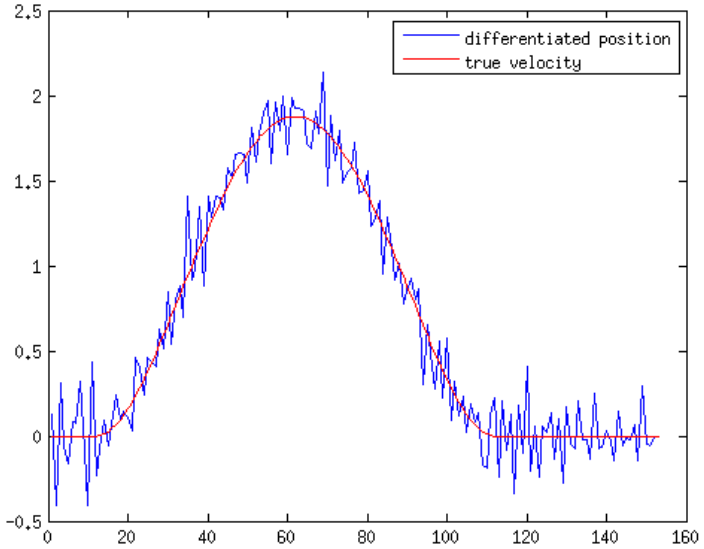

Figure 54. Kalman Filtered Output Charts Example [6].

Avionics – Communication

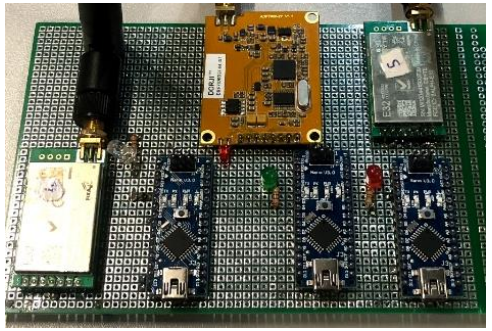

Figure 55. Ground station.

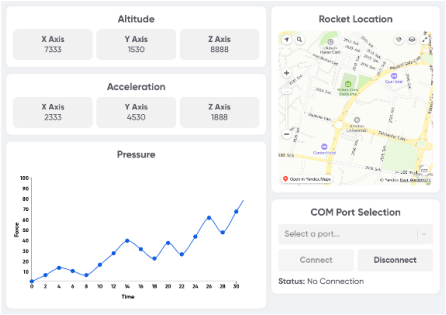

Figure 56. Telemetry Interface.

In the ground station, there are three Arduino Nanos. There is no link between the processors, which ensures that the data does not get jumbled up. The main computer sends pressure, acceleration, and location data to the LoRa SX1278s' ground station, while the backup computer sends pressure and position data to the DRF7020D27 ground station. The data for the referee ground station will be sent by connecting the RGS device to the computer with data from the avionics. As a result of the telemetry band calculations [12], the main avionics will use the LoRa SX1278 module with an 8-kilometer range running in 433 MHz bands, while the backup avionics will use the DRF7020D27 module with a 5-kilometer range working in 433 MHz bands. Antennas TX433-JKD-20P are used.

Telemetry Package Structure

<PACKAGE NUMBER>;< TEAM ID >;<ALTITUDE>;<GPS ALTITUDE>;<GPS LATITUDE>;<GPS LONGITUDE>;<MAIN AVIONIC PRESSURE>;<MAIN AVIONIC Y-AXIS ACCELERATION>;<BACKUP AVIONIC PRESSURE>

(ANNEX-8 RGS has been taken into account in the package structure, the requested data will be forwarded to RGS.) The data packet is the final packet consisting of a combination of avionics.

Link Budget Calculation [7]

$P_{RX} = P_{TX} + G_{TX} - L_{TX} - L_{FS} - L_M + G_{RX} - L_{RX}$

P_{RX} (dBm) = Received Power

P_{TX} (dBm) = Transmitter Power Output

G_{TX} (dBm) = Transmitter Antenna Gain

L_{TX} (dBi) = Loses from Transmitter (Cable)

L_{FS} (dB) = Free-Space Loss

L_M (dB) = Polarization Losses

G_{RX} (dBi) = Receiver Antenna Gain

L_{RX} (dB) = Loses from Receiver (Cable)

L_{FS} = 32.48*log(Frequency(Mhz) + 20 log(Distance(km))

L_M (dB) = 6 dBm (default accepted)

Main Avionic Link Budget:

Free-Space Loss=32.48*log(433)+20log(10) = 103.6

P_{RX} (dBm) = 20 + 4 - 1 - 103,6 - 6 + 4 – 1 = -83.6 dBm

(Since the LoRa SX1278 used can go up to -138 dBm, the distance can be increased.)

Backup Avionic Link Budget:

Free-Space Loss=32.48*log(433)+20log(5) = 99.6

P_{RX} (dBm) = 27 + 4 - 1 – 99,6 - 6 + 4 – 1 = -72.6 dBm

(DRF7020DRF can go up to -117 dBm, the distance can be increased.)

Avionics Prototype Test

Table 23.1. Avionics Prototype Test.

Test Name	Test Location	Test Method	Test Rigs	Data from the Test	Interpretation of Test Data
Avionic Algorithm Test	Altinbas University Mahmutbey Campus	The coding and components of the main avionics and spare avionics computer components will be installed on the perforated plate, and the pressure will be reduced by vacuuming in the airtight container, and then air will be slowly reintroduced. The assembly will also slowly move upwards with 0 horizontally at its apex.	Avionic computer components, Airtight container, Vacuum machine, Buzzer.	The data of the sensors at minimum and 500 meters pressure, the data of the IMU sensor on the Y-axis and the buzzer data.	The success of the BME280, BMP180 pressure sensors in the separation processes and the first separation success with the Y-axis acceleration of the MPU6050 IMU sensor will be observed by the operation of the 5V Buzzer if the outputs are correct.
Card Functionality Test	Altinbas University Mahmutbey Campus	The test setup to be used in the Avionic Algorithm test will also be sent to the ground station by telemetry and the data outputs of the components will be displayed on the computer screen.	Avionic computer components, Airtight container, Vacuum machine, Buzzer, Laptop	Data outputs of the data in the application in the Avionic Algorithm Test on the computer screen.	By observing the data outputs in the Avionic Algorithm Test on the computer screen, it will be observed how fast the incoming data comes and how well the components work.
Communication Distance and Speed Test	Open area	Telemetry of the main avionics and backup avionics computers will be placed at a distance of kilometers from the ground station.	2 LoRa SX1278 and 2 DRF7020F27 telemetry modules (two each for avionic computers and ground station), Laptop	LoRa SX1278 maximum distance and maximum speed data, DRF7020D27 maximum distance and maximum speed data.	It will be observed how far the telemetry modules can receive maximum data in the open area and how fast they receive the data.
Activation of Seperation System Test	Altinbas University Mahmutbey Campus	Parachute components are brought to a certain distance, the pins to which the servo motor is connected will be activated at the time of fall, and the process of opening a parachute with the servo motor will be performed.	Avionics computer components, parachute, servo motor	Servo motor 1 and 0 data.	With the command given to the avionics computers, it will be observed whether the servo motor is successful in opening the parachute, how many degrees of angle and rotation time the servo motor will be successful.

Avionics Prototype Test

Table 23.2. Avionics Prototype Test.

Test Name	Test Location	Test Method	Test Rigs	Data from the Test	Interpretation of Test Data
Tests to be Performed After the Critical Design Report					
Ground Station Interface Test	Altinbas University Mahmutbey Campus.	The data sent to the ground station will be sent to the application prepared by the EVA X Team.	2 Arduino Nano, LoRa SX1278, DRF7020D27, Laptop	In-app data made for telemetry.	It will be observed how healthy the data displayed on the serial screen at the ground station appear in the application made by the EVA X team, and how accurate and fast the application works.
Battery Duration Test	Altinbas University Mahmutbey Campus.	Batteries to be used separately in avionic computers will remain connected to the avionic computers and in working condition and will output to the serial screen as long as it remains on.	2 GP GP1604AU Alkaline Batteries, main avionics, backup avionics	Data on battery operation on the serial screen of the main avionics and backup avionics computers.	It will be observed how long the batteries connected to the avionic computers work differently.
Avionic Temperature Test	Altinbas University Mahmutbey Campus.	The temperature of avionic computers connected with batteries with different wiring will be measured.	2 GP GP1604AU Alkaline Batteries, main avionics computer, backup avionics computer, thermometer	Thermometer data	With the value read from the thermometer, it will be observed how hot the avionic computers are and what precautions should be taken.

Table 24. Avionics Prototype Test Schedule.

	Test Name	April	May			June	
		25th	1st	6th	10th	21st	2nd	7th
1	Avionic Algorithm Test							
2	Card Functionality Test							
3	Communication Distance and Speed Test							
4	Activation of Seperation System Test							
5	Ground Station Interface Test							
6	Battery Duration Test							
7	Avionic Temperature Test							

In the shared test calendar, green boxes indicate the tests completed during the CDR phase, and the red-colored boxes indicate the tests to be performed after the CDR.

Avonics Prototype Video Test: [Avionics Prototype Test YouTube link will be placed here]

Budget

Table 25. Total Budget Approximation.

	Feature	Material	Amount	Price
Avonic System	Lora module SX 1278	-	2	222 TL
	ATmega2560	-	2	333 TL
	MPU6050 IMU Sensor	-	1	43 TL
	BMP180 Barometer	-	1	57 TL
	DRF7020D27 Telemetry Module	-	2	683 TL
	GY-NEO 8M GPS	-	1	426 TL
	BME280 Sensor	-	2	201 TL
	Grove - GPS (Air530)	-	1	263 TL
	Buzzer	-	2	6 TL
	TX433-JKD-20P 433 MHz	-	4	106 TL
	GP GP1604AU Alkaline Battery	-	2	47 TL
Recovery System	Parachutes	Ripstop Nylon	3	1570 TL
	CO_2/Piston System	Aluminum	2	900 TL
Total Price	-	-	-	Around 2600 TL

	Feature	Material	Amount	Price
Body	Nose Cone	E-Glass Fiber/Epoxy and Aluminum	1	600 TL
	Primary Frame	E-Glass Fiber/Epoxy	1	3500 TL
	Main Frame	E-Glass Fiber/Epoxy	1	3500 TL
	Fins	E-Glass Fiber	3	1000 TL
	Coupler	E-Glass Fiber/Epoxy	1	900 TL
	Boat-Tail and Retainer	Aluminum	1	800 TL
Engine System	M2020 Motor	-	1	(Provided by teknofest)
	Inner Motor Tube	E-Glass Fiber/Epoxy	1	1500 TL
	Engine Block	Aluminum	1	200 TL
PAYLOAD	Lora module SX 1278	-	2	222 TL
	ATmega328PU	-	1	193 TL
	TX433-JKD-20P 433 MHz	-	2	106 TL
	GP GP1604AU Alkaline Battery	-	1	47 TL
	BME280 Sensor	-	1	201 TL
	Grove - GPS (Air530)	-	1	263 TL

Checklist

EVA X Checklist					
No	Requirement Item No	Requirement	Recompense Status	PDR Slide Number	Explanation
1	3.1.6.	Mixed teams comprising members from different education/training institutions can participate in the competition.		Slide 2.	
2	3.1.9	Teams shall comprise a minimum of six (6) and a maximum of ten (10) people. A maximum of 6 members can be present in the area.		Slide 2.	
3	3.1.11.	Each team must participate in the competition with one (1) advisor. The requirements related to the team advisor are given in the relevant article.		Slide 2.	Advisor requirements are attached in the zip file in PDF format.
4	3.1.17.	A flight simulation report shall be prepared and delivered in both the PDR and CDR stages.		Slide 9.	FSR is attached in the zip file in PDF format.
5	3.1.22.	The teams are responsible for listing all team members that will participate in the competition and the team advisor in all the reports (PDR, CDR, LRR, PLER) they prepare.		Slide 2.	
6	3.1.24.7.	The faculty member/academic advisors to university teams must be an academician (research assistant, lecturer) in any faculty in the field of Engineering and Science, or an academician of any field who has previously participated in rocket competitions in the country or abroad.		Slide 2.	
7	3.1.25.	The team must have a team captain.		Slide 2 .	
8	3.2.1.3.	The rockets in the Medium- and High-Altitude Categories must carry out the operation concept given in Figure 1 as an example.		Slide 3 to 5.	Operation concept shown in slide 5 with all the competition rules in mind.
9	3.2.1.4	Rockets must release the payload at the apogee point and deploy the drogue parachute (yellow drag parachute in Figure 1).		Slide 5,33.	
10	3.2.1.5	Main parachute will be deployed at a maximum of 600 m and a minimum 400 m from the ground.		Slide 5.	
11	3.2.1.20	The payload will be recovered separately from the rocket, whereas the rocket parts will all be recovered together. There shall be a system (GPS, radio transmitter) pinpointing the locations of both the payload and the parts in question.		Slide 37.	
12	3.2.1.21.	Teams are required to make flight simulations in accordance with the “Open Rocket Simulation” menu (Figure 3). Teams that have not included the simulation described in Figure 3 in their Open Rocket file shall not be evaluated.		Slide 5.	An ork. file has also been attached in the zip file with figure 3 simulation applied.
13	3.2.1.23.	Teams shall not enter their Payload as "Unspecified Mass". The payload shall be named "PAYLOAD", and its mass shall be entered as 4000 grams (4 kg) minimum as a single piece. The values on the "Launch Simulation" screen seen in Figure 3 should be entered into the simulation. Teams that fail to carry out the simulation using these values shall be disqualified.		Slides 3,38.	
14	3.2.3.1.	The system of parachute must be used for the recovery system.		Slide 35,36 .	
15	3.2.2.2.	In order to prevent damage to the rocket and its parts, the velocity of the loads carried by the main parachute must be 9 m/s maximum and 5 m/s minimum.		Slide 36.	

Checklist

16	3.2.2.3.	The drogue parachute must be able to prevent the rocket from tumbling. This parachute must reduce the descent rate of the rocket to a rate not be less than 20 m/s.		Slide 35.	
17	3.2.2.5	The Payload must be landed “independently” with its own parachute, without any connection to the rocket parts (no equipment such as shock cord connecting to any point).		Slide 33.	
18	3.2.2.13.	Each parachute will be distinctly colored and easily distinguished by the naked eye from a distance (it is of crucial importance that the parachutes not be white, blue or any shades of these colors).		Slide 35.	
19	3.2.3.1.	The payload must have a mass of at least four (4) kilograms.		Slide 38.	
20	3.2.3.4.	The payload, which is separated from the rocket at the apogee in the Medium-Altitude category, must transmit the pressure, temperature, and humidity data of the atmosphere to the ground station at a frequency of 5 Hz (5 units of data every second for each data group).		Slide 37.	
21	3.2.4.1	Rockets that will compete in the High School, Medium-Altitude and Challenging Task categories must fly at subsonic (below Mach 1) speeds.		Slide 4.	
22	3.2.4.3.	The maximum outer diameters of all parts of the rocket must be of the same value (Stages of different diameters and diameter changes between stages are not allowed. Boat-Tail use is allowed in line with rail positioning restrictions.)		Slide 4.	
23	3.2.4.7.	The minimum rail exit velocities are as follows: 15 m/s in the High School Category, 25 m/s in the Medium-Altitude Category, 30 m/s in the High-Altitude Category and 20 m/s in the Challenging Task Category.		Slide 5.	
24	3.2.5.1.	The internal and external pressure of the rocket must be in balance. To ensure pressure balance, a minimum of three (3) holes with diameters of 3.0–4.5 mm must be located between the nose cone and the frontal part of the body tube, in the body tube part housing the avionics systems, and in the body tube section between the rear part of the body tube and the engine.		Slide 17,20 .	
25	3.2.5.5.	Nose cone shoulder must have a diameter of at least one and a half (1.5) times the outer diameter of the body tube. Couplers are expected to have a diameter of at least 0.75 times each of the outer diameter of the body tubes into which they will be integrated. Failure to comply is grounds for disqualification. A sample nose cone shoulder is provided in Figure 4 and sample coupler is provided in Figure 5.		Slide 12 .	
26	3.2.5.7.	The rail buttons must be attached to the structurally reinforced parts of the body tube. Each rocket must have a minimum of two (2) rail buttons. One should be located on the engine area, between the engine centre of gravity and the end of the body tube. The centre of gravity of the rocket must be between the two rail buttons.		Slide 20.	
27	3.2.5.10.	The flight computer and all switches on the payload must be located at most 2500 mm ahead of the rocket nozzle (Figure 6).		Slide 17,20 .	
28	3.2.6.1.	The deployment and recovery systems found on the rocket are managed by the flight control computer.		Slide 33.	
29	3.2.6.2.	The communication computer that ensures the transmission of telemetry data to the ground station can operate either standalone or integrated with the Flight Control Computer.		Slide 60.	
30	3.2.6.7.	In the Medium-Altitude category, the use of at least two (2) flight control computers is mandated. At least one (1) of these flight control computers must be an authentic flight-control computer. At least one (1) of the flight control computers used must provide the utility of a communication computer.		Slide 46.	
31	3.2.6.9.	No electrical or wireless connection is permitted between the flight control computers used in the system.		Slide 47.	
32	3.2.6.10.	The flight control computers must be completely independent of each other. Each computer must have its own processor, sensors, power source and cabling.		Slide 46,47.	
33	3.2.6.11.	The flight control computers used are connected to the deployment system actuator via electric lines, cables etc. (each line should be independent).		Slide 37.	
34	3.2.6.12.	In the event of the partial or complete failure of one of the flight control computers and/or one of the systems to which they are connected, the others must be able to perform the rocket's recovery functions without interruption.		Slide 52,58.	

Checklist

35	3.2.6.13.	The flight control computers must have at least two (2) sensors, and data from these sensors must be used in the flight control algorithm.		Slide 46.	
36	3.2.6.14.	There must be at least one (1) barometric pressure sensor in all flight control computers.		Slide 46.	
37	3.2.6.15.	In the event of two (2) barometric pressure sensors being used in the flight control computers, the sensors must be different from each other (Sensors used in different flight control computers may be the same as each other).		Slide 46.	
38	3.2.6.16.	In the flight control algorithm, the deployment system must not be triggered by data from GPS.		Slide 47,49,55.	
39	3.2.6.20.	All teams must have a ground station to receive real-time data from their rockets and payloads.		Slide 60.	
40	3.2.6.21.1	To launch the recovery of the rockets, the location data of the rocket must have been transmitted to the Ground Station in real time.		Slide 60.	
41	3.2.6.22.	The fact that rocket parts will land far away from the ground station should be considered, and the range of the transceiver antennae should be chosen taking the flight trajectory of the rocket into account.		Slide 60.	
42	3.2.6.23.	The link bandwidth must be budgeted by assessing the power of the RF module, and this must be presented in the relevant design reports.		Slide 60-.	
43	3.2.6.26.	In the design and production of the rocket, it must be ensured that power can be supplied to the flight control computers from outside the body tube (for example, there should be an accessible switch on the body tube). The starting of systems by using tools with ropes, shunts or screwdrivers etc. will not be permitted.		Slide 20.	
44	3.2.6.21.1	To launch the recovery of the rockets, the location data of the rocket must have been transmitted to the Ground Station in real time.		Slide 60.	
45	3.2.6.22.	The fact that rocket parts will land far away from the ground station should be considered, and the range of the transceiver antennae should be chosen taking the flight trajectory of the rocket into account.		Slide 60.	
46	3.2.6.23.	The link bandwidth must be budgeted by assessing the power of the RF module, and this must be presented in the relevant design reports.		Slide 60.	
47	3.2.6.26.	In the design and production of the rocket, it must be ensured that power can be supplied to the flight control computers from outside the body tube (for example, there should be an accessible switch on the body tube). The starting of systems by using tools with ropes, shunts or screwdrivers etc. will not be permitted.		Slide 20.	
48	3.2.6.28	Design and production must be done in such a way that power can be supplied to the electronic circuits on the Payload from switches on the body tube of the rocket.		Slide 38.	
49	3.2.6.33.	At least two criteria that will trigger split sequences in the flight algorithms must be determined.		Slide 52,58.	
50	3.2.6.34.	Decision-making parameters must be based on the data read from the sensors.		Slide 52,58.	
51	3.2.6.35.	The data read from the sensors must not be used directly, and any incorrect reading or sensor error must be taken into account. The measures to be taken in such situations (such as filtering) must be explained in detail in the relevant design reports.		Slide 53,59.	
52	4.3.1	The teams are responsible for carrying out and providing the results of all the necessary analyses and tests in the Critical Design Report (CDR), demonstrating that their designs are ready to proceed to the final production, integration and testing phases.		Slide 42 to 45.	
53	4.3.6	The system should be explained with an integration scheme (i.e. assembly details of the systems must be presented with supporting visuals from the CAD program, answering such questions as “How the stages are connected to each other, in the Challenging Task category”, “How the nose cone is connected to the body tube", “How the parachute is connected to the body tube”, “How the motor is fixed inside the body tube in such a way that it can be removed”).		Slide 28.	
54	4.3.12.	Open Rocket files with an “.ork” extension supporting the report must be submitted with the report.		Slide 3 to 5.	
55	4.3.17.	All electronic components on the system powered by batteries shall be specified in the CDR, which should include switching circuit schematics.		Slide 50,56.	

FMEA
Error Types and Effects analysis

A Failure Modes and Effects Analysis (FMEA) is located in a zip file in excel format.

References

[1] Benson, T. (n.d.). Velocity during recovery. NASA. Retrieved May 5, 2022, from https://www.grc.nasa.gov/www/k-12/VirtualAero/BottleRocket/airplane/rktvrecv.html#:~:text=Velocity%20During%20Recovery,recovery%20portion%20of%20the%20flight.

[2] Engineering ToolBox, (2003). U.S. Standard Atmosphere vs. Altitude. Retrieved February 19, 2022, [online] Available at: https://www.engineeringtoolbox.com/standard atmosphere d_604.html .

[3] Crowell Sr., G. A. (1996). The Descriptive Geometry of Nose Cone .

[4] ÇAYIROĞLU, İ. (2012). Kalman Filtresi ve Programlama. http://www.ibrahimcayiroglu.com/.

[5] Roi YozevitchRoi Yozevitch 13733 silver badges99 bronze badges, & AntonAnton 4. (1967, August 1). Kalman filter convergence. Stack Overflow. Retrieved May 5, 2022, from https://stackoverflow.com/questions/59046355/kalman-filter-convergence .

[6] Kalman filter velocity estimation example. KF Velocity Estimation Example. (n.d.). Retrieved May 5, 2022, from https://www.cs.cmu.edu/~cga/dynopt/kalman/kalman.html

[7] Pozar, D. M. (2012). *Microwave engineering*. Joh Wiley & Sons, Inc.

[8] T P, Sathishkumar & Satheeshkumar, S & Jesuarockiam, Naveen. (2014). Glass fiber-reinforced polymer composites - A review. Journal of Reinforced Plastics and Composites. 33. 1258–1275. 10.1177/0731684414530790.

[9] Pardini, L.C., & Gregori, M.L. (2010). Modeling elastic and thermal properties of 2.5D carbon fiber and carbon/SiC hybrid matrix composites by homogenization method. Journal of Aerospace Technology and Management, 2, 183-194.

References

[10] Papastathis, T. & Bakker, Otto Jan & Ratchev, Svetan & Popov, A.. (2012). Design Methodology for Mechatronic Active Fixtures with Movable Clamps. Procedia CIRP. 3. 323–328. 10.1016/j.procir.2012.07.056.
[11] Alam, Ashraful & Yadama, Vikram & Cofer, William & Englund, Karl. (2012). Analysis and evaluation of a fruit bin for apples. Journal of Food Science and Technology -Mysore-. 51. 10.1007/s13197-012-0889-3.
[12] Tuset-Peiro, Pere & Angles, Albert & Lopez Vicario, Jose & Vilajosana, Xavier. (2014). On the suitability of the 433 MHz band for M2M low-power wireless communications: Propagation aspects. European Transactions on Telecommunications. 25. 10.1002/ett.2672.